

AD/A 007 141

STRAIN RATE EFFECTS IN BRITTLE AND TOUGH MATERIALS

ARMY MATERIALS AND MECHANICS RESEARCH CENTER

DECEMBER 1974

DISTRIBUTED BY:

**NTIS**

National Technical Information Service  
U. S. DEPARTMENT OF COMMERCE

MS

findings in this report are not to be construed as official Department of the Army position, unless so designated by other authorized documents.

tion of any trade names or manufacturers in this report  
l not be construed as advertising nor as an official  
orsement or approval of such products or companies by  
United States Government.

DISPOSITION INSTRUCTIONS

Destroy this report when it is no longer needed.  
Do not return it to the originator.

UNCLASSIFIED

SECURITY CLASSIFICATION OF THIS PAGE (When Data Entered)

REPORT DOCUMENTATION PAGE		READ INSTRUCTIONS BEFORE COMPLETING FORM
1. REPORT NUMBER AMMRC TR 74-34	2. GOVT ACCESSION NO.	3. RECIPIENT'S CATALOG NUMBER DA 044735
4. TITLE (and Subtitle) STRAIN RATE EFFECTS IN BRITTLE AND TOUGH MATERIALS		5. TYPE OF REPORT & PERIOD COVERED Final Report
7. AUTHOR(s) Milton M. Mardirosian		6. PERFORMING ORG. REPORT NUMBER
9. PERFORMING ORGANIZATION NAME AND ADDRESS Army Materials and Mechanics Research Center Watertown, Massachusetts 02172 AMXMR-ER		8. CONTRACT OR GRANT NUMBER(s)
11. CONTROLLING OFFICE NAME AND ADDRESS U. S. Army Materiel Command Alexandria, Virginia 22333		10. PROGRAM ELEMENT, PROJECT, TASK AREA & WORK UNIT NUMBERS D/A Project: 1T062105A328 AMCMS Code: 502E.11.29400 Agency Accession: DA QA4735
14. MONITORING AGENCY NAME & ADDRESS (if different from Controlling Office)		12. REPORT DATE December 1974
		13. NUMBER OF PAGES 41
		15. SECURITY CLASS. (of this report) Unclassified
		15a. DECLASSIFICATION/DOWNGRADING SCHEDULE
16. DISTRIBUTION STATEMENT (of this Report)  Approved for public release; distribution unlimited.		
17. DISTRIBUTION STATEMENT (of the abstract entered in Block 20, if different from Report)  Reproduced by NATIONAL TECHNICAL INFORMATION SERVICE U.S. Department of Commerce Springfield, VA. 22151		
18. SUPPLEMENTARY NOTES		
19. KEY WORDS (Continue on reverse side if necessary and identify by block number)  Steels                      Strain rate Titanium alloys          Temperature distribution Uranium alloys          Mechanical properties		
20. ABSTRACT (Continue on reverse side if necessary and identify by block number)  (SEE REVERSE SIDE)		

PRICES SUBJECT TO CHANGE (40)

DD FORM 1 JAN 73 1473

EDITION OF 1 NOV 65 IS OBSOLETE

UNCLASSIFIED

SECURITY CLASSIFICATION OF 5 PAGE (When Data Entered)

UNCLASSIFIED

SECURITY CLASSIFICATION OF THIS PAGE(When Data Entered)

Block No. 20

ABSTRACT

Strain rate sensitivity effects and strain hardening characteristics at room, elevated, and subzero temperatures were evaluated for a wide variety of both tough and brittle materials including 4340, 52100, and HF-1 steels, 6Al-4V and 6Al-6V-2Sn titanium alloys and the 8Mo-1/2Ti uranium alloy. Mechanical property parameters such as true stress, true strain, true fracture stress, ultimate and yield strengths, tension modulus, and reduction of area are examined under a temperature environment ranging from -116 C to +260 C over a strain rate spectrum of  $10^{-3}$   $\text{sec}^{-1}$  to  $5 \times 10^2$   $\text{sec}^{-1}$ . (Author)

10

UNCLASSIFIED

SECURITY CLASSIFICATION OF THIS PAGE(When Data Entered)

## CONTENTS

	Page
INTRODUCTION. . . . .	1
EXPERIMENTAL PROCEDURE. . . . .	1
SPECIMEN MATERIALS AND GEOMETRY . . . . .	3
HEAT TREATMENT AND MECHANICAL PROPERTIES. . . . .	3
STRAIN RATE BEHAVIOR. . . . .	7
CONCLUSIONS . . . . .	28
ACKNOWLEDGMENT. . . . .	31
APPENDIX A. TABULATION OF TEST DATA AND TRUE STRESS-TRUE STRAIN RESULTS	
Table A-1. EXPERIMENTAL TEST DATA AT ROOM TEMPERATURE . . . . .	33
Table A-2. EXPERIMENTAL TEST DATA TAKEN AT VARYING TESTING TEMPERATURES . . . . .	34
Table A-3. TRUE STRESS-TRUE STRAIN RESULTS AT ROOM TEMPERATURE. . .	35
Table A-4. TRUE STRESS-TRUE STRAIN RESULTS TAKEN AT VARYING TESTING TEMPERATURES . . . . .	36

## INTRODUCTION

Although the actual relationship between mechanical properties of materials and rate of loading becomes quite involved, it can be postulated that, in general, mechanical properties are sensitive to strain rate effects. However, it is generally acknowledged that the movement of dislocations accounts for the strain rate effects.<sup>1</sup>

Dislocation locking<sup>2</sup> is another phenomenon which can affect mechanical properties and is subject to strain rate behavior. It is believed that dislocations can be locked by segregate atoms and that plastic flow will not occur until mobile dislocations are formed. Some finite period of time is required before sufficient dislocations are formed to cause observable plastic deformation. The time delay associated with this phenomenon causes an increase in the upper yield point which is logarithmically related to strain rate.

In addition, Hoge<sup>3</sup> indicated that stress corrosion is affected by strain rate interactions in uranium alloys. The stress corrosion effect predominates at relatively slow strain rates, i.e., up to approximately  $1.0 \text{ sec}^{-1}$ , whereas at faster loading rates there is insufficient time for any appreciable corrosive action. As the loading time is decreased (higher strain rates), the yielding phenomenon is delayed and ultimate strength increases.

In this report, the effects of strain rate at various temperature levels on the mechanical properties of selected brittle and tough materials are studied. Strain rate sensitivity evaluations for these materials are determined as a function of the maximum range of strain rates investigated.

## EXPERIMENTAL PROCEDURE

Dynamic tension tests were conducted\* using a 10,000-pound Universal Tester (Plastechon Model 591) in conjunction with bonded resistance foil-type strain gage† techniques and a dual-beam oscilloscope. A relatively high natural frequency piezoelectric transducer (60 kHz) for load readout purposes was incorporated in this commercial machine which was modified slightly with the installation of a triggering device to record the transient strain-time and load-time oscillographic traces.

In operation, hydraulic power is supplied to the servo-controlled, electro-hydraulic testing machine through a 3000-psi 7.5-gpm pump driven by a 15-hp electric motor. A sketch of the essential components is shown in Figure 1. The movable ram is actuated by a dual-lead continuous film potentiometer with a 6-inch stroke.

\*The testing phase of this study was carried out under contract at Plas-Tech Equipment Company, Natick, Massachusetts.

†Micro-Measurements Type EP-03-250-BC-120.

1. DORN, J. E., MITCHELL, J., and HAUSER, E. *Dislocation Dynamics*. Exp. Mechanics, November 1965.

2. HAHN, G. T. *A Model for Yielding with Special References to the Yield Point Phenomena of Iron and Related BCC Metals*. Acta Met., v. 10, 1962.

3. HOGG, K. E. *Some Mechanical Properties of Uranium - 10% Mo Alloy Under Dynamic Tension Loads*. Lawrence Radiation Laboratory, Livermore, California, UCRL 12357. Rev. 1, February 1965.

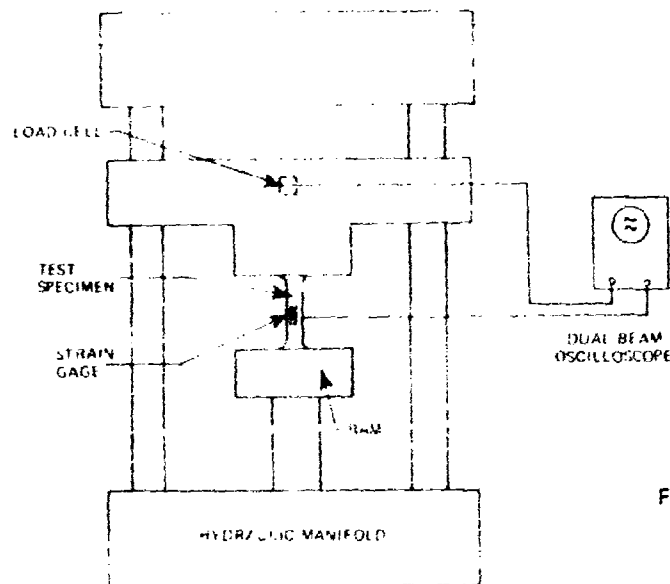


Figure 1. Test setup

The load signal is generated by a quartz-type strain-gage force transducer mounted directly behind the test specimen. Two axial strain gages, mounted on opposite sides of the reduced section of the specimen, give an accurate measurement of the initial strain and permit the determination of elastic modulus and yielding behavior.

Just as the ram begins to accelerate, it contacts a trigger pin, starting the oscilloscope sweep. The signals, both from the load cell and from the test specimen strain gages, are displayed on a dual-beam oscilloscope and photographed. These data provide a load-time and strain-time record of the event.

True stress and true strain were calculated from the portion of the engineering stress-strain curves, developed from the load-time and strain-time oscillographic traces, up to ultimate load and from the specimen measurements after fracture. The stress and deformation characteristics of the various test materials were determined from the following expressions:

$$(1) \text{ true stress (psi)} = \sigma (1 + \epsilon)$$

$$(2) \text{ true strain} = \ln (1 + \epsilon)$$

$$(3) \text{ true fracture stress (psi)} = L_f/A_f$$

$$(4) \text{ true strain at fracture} = \ln (A_0/A_f)$$

where

$\sigma$  = yield or ultimate stress, psi, calculated from load-time oscillographic records

$\epsilon$  = corresponding strain, in./in. from strain-time oscillographic records

$L_f$  = applied load, pounds, at fracture from load-time oscillographic records

$\ln$  = Napierian logarithm =  $\log_e$

$A_0$  = original cross-sectional area, sq in., of test specimen at reduced section

$A_f$  = fractured area, sq in., of test specimen at reduced section

A correction for the triaxial stress state in the neck<sup>4</sup> region of the test specimen was not applied. True stress-strain curves are plotted assuming a smooth interpolation between the regions of ultimate load and fracture. The nominal strain rate was graphically obtained from the strain-time relationships immediately prior to the ultimate load value.

### SPECIMEN MATERIALS AND GEOMETRY

All strain-rate behavioral tests were conducted with cylindrical 0.15"-diameter specimens of the configuration shown in Figure 2.

The materials analyzed were 4340, 52100, and HF-1 alloy steels, 6Al-6V-2Sn and 6Al-4V titanium alloys, and 8Mo-1/2Ti uranium alloy. The titanium alloy specimens were taken from forged bars, whereas the 4340 and 52100 specimens were machined from hot-rolled bar stock. The HF-1 steel specimens were extracted from forged shell bodies of 105-mm size while the uranium specimens were removed from a hollow, backward extruded cylinder which was sliced into 120 degree sections and forged flat at 1200 F. All specimens, with the exception of the uranium ones, were taken longitudinal to the material grain flow.

### HEAT TREATMENT AND MECHANICAL PROPERTIES

The composition and mechanical properties for each material are presented in Tables 1 and 2 and their corresponding heat treatments are shown in Table 3.

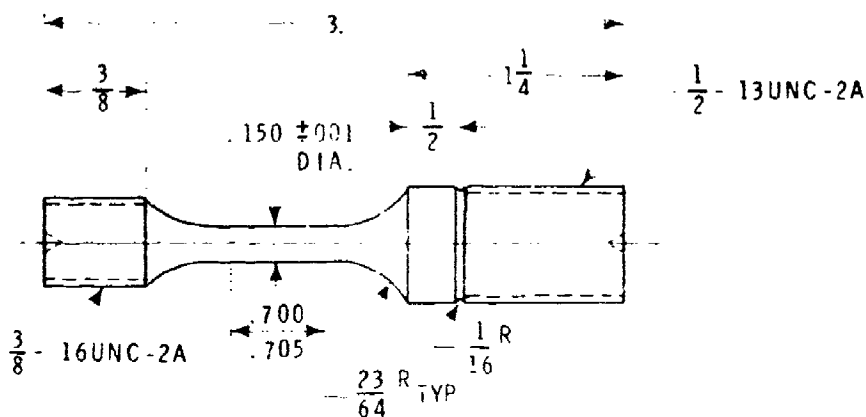


Figure 2. Test specimen

4. BRIDGMAN, P. W. *The Stress Distribution at the Neck of a Tension Specimen*. Transactions, Am. Soc. Metals, v. 32, 1944, p. 553-574.

Table 1. CHEMICAL COMPOSITION  
(in weight percent)

Material	C	Mn	Ni	Cr	Mo	Si	P	S
<b>Steel Alloys</b>								
4340 Q&T	0.41	0.78	1.74	0.85	0.24			
52100-1 IQ&T(1000)	1.0	1.35		1.50				
52100-2 IQ&T(1200)	1.0	1.35		1.50				
52100-3 Norm&T	1.0	1.35		1.50				
HF-1 (Type 1)	1.07	1.78				1.05	0.01	0.016
HF-1 (Type 2)	1.11	1.80				1.04	.01	.017
HF-1 (Type 3)	1.09	1.80				1.05	.01	.017
<b>Titanium Alloys</b>								
	C	Al	V	Sn	Fe	Cu		
6Al-4V	0.03	6.12	4.30					
6Al-6V-2Sn	.09	5.53	5.84	1.88	0.61	0.79		
<b>Uranium Alloy</b>								
	C	Mo	Ti	Fe	Si	N	O	H
8Mo-1/2Ti	0.006	7.92	0.45	0.0654	0.02	0.0004	25ppm	0.5ppm

Table 2. NOMINAL MECHANICAL PROPERTIES

Material	Y.S. 0.1 ksi	T.S. ksi	R.A. %	Impact Energy ft-lb -40 F
<b>Steel Alloys</b>				
4340 Q&T	141	153	64	24.0
52100-1 IQ&T(1000)	181	186	11	2.3*
52100-2 IQ&T(1200)	142	173	21	3.2*
52100-3 Norm&T	134	209	8	3.4*
HF-1 (Type 1)	105	156	24.8	3.1
HF-1 (Type 2)	122	160	25.7	3.7
HF-1 (Type 3)	82	138	5.8	2.1
<b>Titanium Alloys</b>				
6Al-4V	149	162	46	8.5
6Al-6V-2Sn	184	190	36	7.5
<b>Uranium Alloy</b>				
8Mo-1/2Ti	135	140	40	3.4

\*Room Temperature Results

The alloy steels selected in this investigation are structural alloys used by the Army for applications involving high strain rates.

The 4340 steel was quenched and tempered to provide a tempered martensitic structure of moderate strength and high toughness typical of properly heat-treated high-strength structural steel.

One heat treatment of 52100 steel involved an austenitize, followed by holding in the two-phase region to precipitate out grain boundary carbides before quenching (IQ&T treatment). The 52100 steel, which is an air-hardening steel, was also normalized and tempered (Norm&T) to produce an alternate microstructure and associated yield/tensile strength ratio without the carbide embrittlement.

For the 52100 steel, the yield strengths and tensile ductility were much lower for the Norm&T treatment than for the IQ&T treatment. The yield strength/tensile strength ratio was much lower, and the reduction of area was quite low.

Table 3. HEAT TREATMENTS

Material	Type	Heat Treatment
Steel Alloys		
4340	Q&T	1550 F 1hr-Oil Quench 1100 F 2hr-Air Cool
52100-1	10&T	1750 F 2hr-Furnace Cool to 1350 F 1-1/2hr-Oil Quench 1000 F 1hr-Air Cool
52100-2	10&T	1750 F 2hr-Furnace Cool to 1350 F 1-1/2hr-Oil Quench 1200 F 1hr-Air Cool
52100-3	Norm&T	1750 F 2hr-Air Cool 500 F 1hr-Air Cool
HF-1	1	1425 F 1-1/2hr-Oil Quench 1100 F 1hr-Air Cool
HF-1	2	1550 F 1-1/2hr-Oil Quench 1150 F 1-1/2hr-Air Cool
HF-1	3	1700 F 1-1/2hr-1150 F hold 1-1/2hr-Air Cool
Titanium Alloys		
6Al-4V	Solution Treated & Aged	1700 F 1hr-Water Quench 1150 F 4hr-Air Cool
6Al-6V-2Sn	Solution Treated & Aged	1550 F 1hr-Water Quench 1050 F 4hr-Air Cool
Uranium Alloy		
8Mo-1/2Ti	Annealed & Forged	1600 F 2hr-Furnace Cool Forge at 1700 F-Air Cool

The steel designated HF-1 was developed for use in ammunition by Bethlehem Steel Company. In view of its possible use at high strain rates, this relatively brittle material has been included in this study. This high carbon steel contains 2% manganese and 1% silicon to provide hardenability and a degree of embrittlement. The types of heat treatment employed also influence the ductility and toughness. The three heat treatments selected for evaluation in this study of HF-1 steel are: (1) an incompletely austenitized structure followed by a quench and temper to produce tempered martensite with pearlite ghosts and grain boundary carbides; (2) a more complete austenitized followed by a quench and temper to produce tempered martensite; (3) an isothermally transformed structure to produce coarse pearlite.

Typical microstructures in HF-1 steel obtained after these treatments, using an electron beam microscope examination of replicas at 10,000X, are shown in Figure 5. The structures of the specimens as a result of treatments 1 and 2 contained considerable amounts of undissolved carbides indicating that the matrix had not been transformed to a homogeneous austenite during the austenitizing operation.

For the HF-1 steel, the tensile strengths after the three heat treatments were similar. These treatments were designed to impart a range of toughness levels. Thus the yield strength/tensile strength ratio was lower for the coarse pearlite and incompletely austenitized quenched and tempered structures than for the tempered martensite structure. The ductility and toughness were also reduced in these two structures.

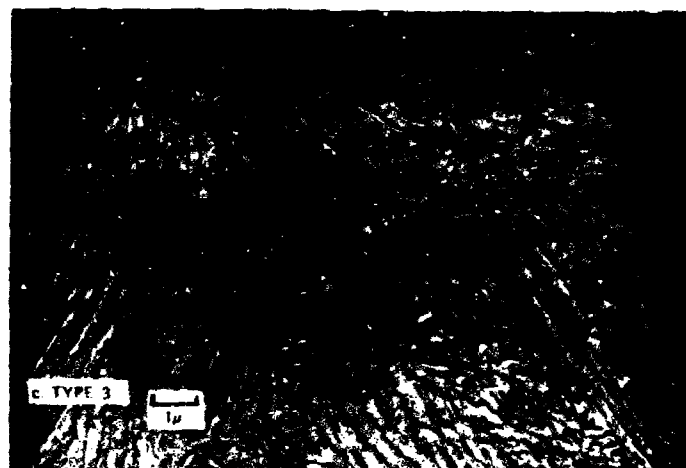
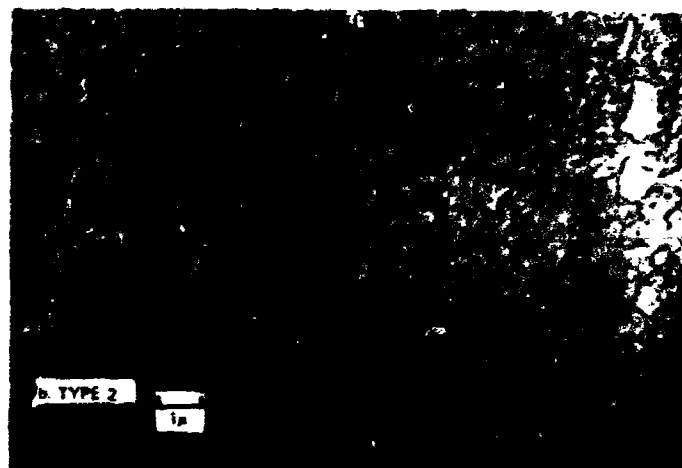


Figure 3. Typical microstructures in HF-1 steel

The mechanical properties obtained in the two titanium alloys and the uranium alloy are typical of the properties of these materials.

### STRAIN RATE BEHAVIOR

There was not a great deal of appropriate information in the literature to assess the results of these strain rate behavioral tests with other methods and other investigators. Consequently, only limited comparisons were possible.

Materials properties parameters such as yield strength, ultimate tensile strength, true fracture stress, tension modulus, and reduction of area are examined under a temperature environment ranging from subzero through elevated temperature (-116 C to +260 C) over a strain rate spectrum of  $10^{-3} \text{ sec}^{-1}$  to  $5.31 \times 10^2 \text{ sec}^{-1}$ .

The strain rate sensitivity of the various brittle and tough materials was determined by correlating the cumulative effects in mechanical property values with strain rate variations. In addition, the strain hardening characteristics of these materials were evaluated from an analysis of the true stress-true strain behavior at a variety of temperature and strain rate conditions. The experimental test data as well as the true stress-true strain results are summarized in tabular form in the Appendix.

Figure 4a shows the data obtained from 4340 steel with respect to yield strength, ultimate tensile strength, true stress at fracture, modulus of elasticity in tension, and reduction of area as a function of strain rate at room temperature (23 C). Four decades of strain rate from  $7.7 \times 10^{-3}$  to  $41.8 \text{ sec}^{-1}$  are covered.

It can be stated that the true fracture stress was fairly constant over the range of strain rates examined. Both the ultimate and yield strengths as well as the tension modulus increased with increasing strain rates, whereas the reduction of area was quite constant.

The increase in ultimate and yield strengths appeared to be fairly uniform; in comparison, a transition point at approximately  $1.0 \text{ sec}^{-1}$  was noted in the behavior of the tension modulus wherein the resultant increase progressed from a moderate rise at strain rates below  $1.0 \text{ sec}^{-1}$  to a rather sharp gain above this transition point.

The results for 52100 steel are shown in Figure 4b. The true fracture stress of this alloy in the three heat-treated conditions studied, in addition to the tension modulus, for the grain boundary embrittled high temper (52100-2) and normalized (52100-3) conditions, behaved monotonically with increased strain rate. For the ultimate strength performance, it is noted that there is a slight decrease with strain rate. However, the actual changes were sufficiently small so that the net change is not considered significant.

The yield strength of the high temper 52100 steel in the IQ&T condition showed a moderate decrease with increasing strain rate; however, for the Norm&T treatment, the yield strength increased moderately with strain rate. The reduction of area,

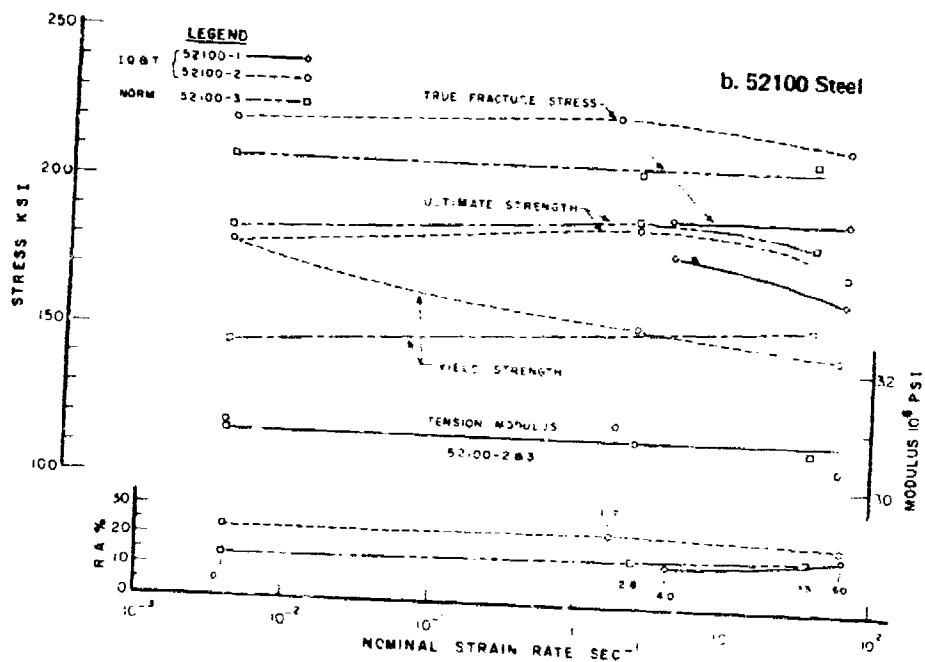
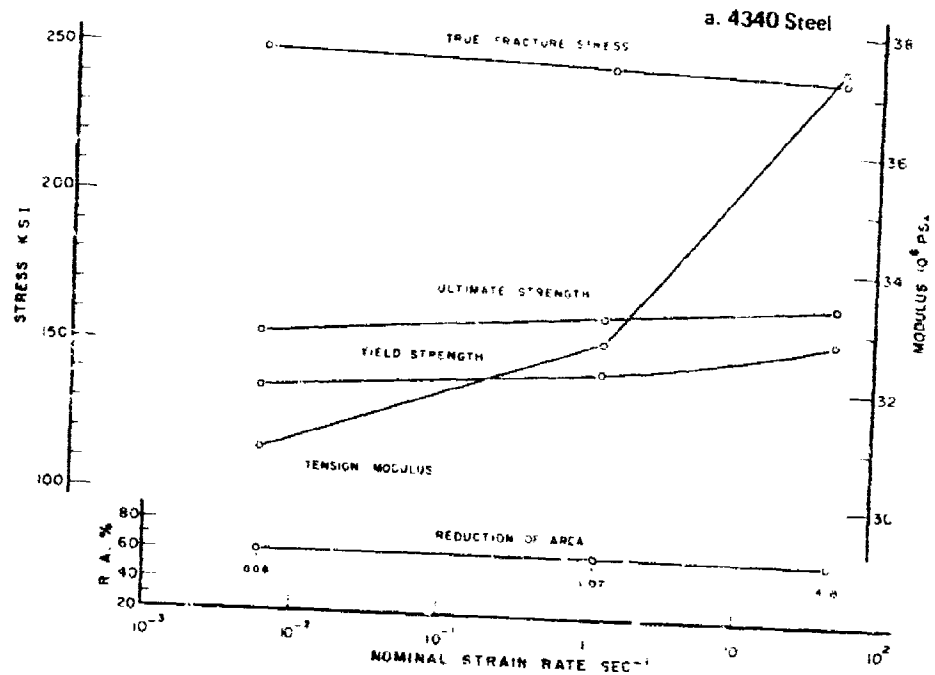


Figure 4. Mechanical properties of tested steels

as in the case of 4340 steel, remained fairly constant for both the grain boundary embrittled (IQ&T) and normalized conditions over the range of strain rates involved.

The relationship of true fracture stress, ultimate tensile strength, yield strength, tension modulus, and reduction of area versus strain rate at both room temperature (23 C) and -116 C for HF-1 steel in the three heat-treated conditions (Types 1, 2, and 3) are presented graphically in Figure 5. The range of strain rates covered in these tests extended from  $10^{-3} \text{ sec}^{-1}$  to  $5.3 \times 10^2 \text{ sec}^{-1}$ .

The behavior of true fracture stress versus strain rate at both room temperature and -116 C is shown in Figure 5a. At room temperature, the three types of HF-1 steel investigated show an increase in fracture stress with increase in strain rate, whereas at -116 C the fracture stress remained constant.

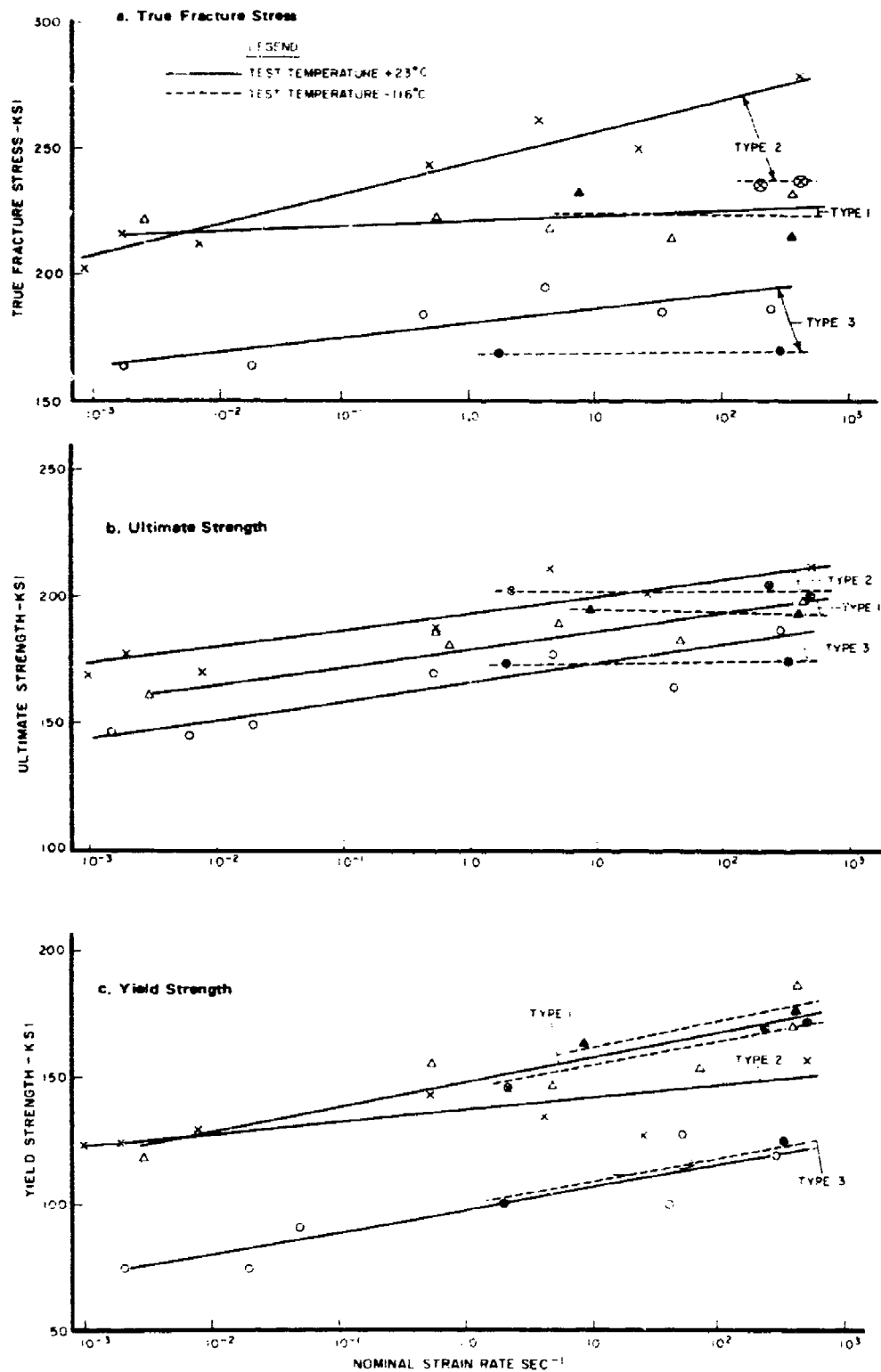
The same phenomenon was demonstrated for the ultimate tensile strength as seen in Figure 5b. At room temperature, essentially three parallel slopes were developed, indicating that the rate of increase of the ultimate strength with increasing strain rate was similar for all three types of HF-1 steel. As with fracture stress, the ultimate strength varied monotonically with strain rate at -116 C.

Figure 5c shows that the yield strengths increased with increasing strain rate at both room temperature and -116 C. However, the rate of increase for the Type 2 material was not as pronounced as with Types 1 and 3, resulting in the fact that above a strain rate of approximately  $4 \times 10^{-2} \text{ sec}^{-1}$ , the yield strength levels for Type 1 exceeded the group at the room temperature condition. In all cases the levels at -116 C were superior to the values obtained at room temperature. This result was in contradiction to that determined for the ultimate and true fracture stress levels at the upper regions of the strain rate spectrum, wherein the values at room temperature in all cases exceeded those obtained at -116 C.

The degree of dependence on strain rate for the tension modulus values is demonstrated in Figure 5d. At both test temperatures the three types exhibited an increase in modulus with increasing strain rate. With the exception of Type 3 material, the rate of increase was much more pronounced at -116 C. The Type 2 material at -116 C yielded the sharpest increase in modulus registering a value of  $39.5 \times 10^6 \text{ psi}$  at the upper limit of the strain rate range (250 to  $500 \text{ sec}^{-1}$ ).

Reduction of area, a parameter for evaluating ductility, behaved monotonically with strain rate at room temperature for all three types of HF-1 steel (Figure 5e) from quasi-static to high-order strain rates ( $530 \text{ sec}^{-1}$ ). At -116 C, Types 2 and 3 were relatively unaffected by strain rate, whereas Type 1 showed a marked decrease in the R.A. value from  $10 \text{ sec}^{-1}$  to approximately  $530 \text{ sec}^{-1}$ .

The results of tests at room temperature (23 C) on the 6Al-6V-2Sn and 6Al-4V titanium alloys are shown in Figure 6. The true fracture stress and ultimate strength for both alloys in the solution-treated and aged condition increased slightly with strain rate up to approximately  $2.4 \text{ sec}^{-1}$ . Above this value there was a marked increase in fracture and ultimate strengths. The yield strengths of both titanium alloys as well as the tension modulus for the 6Al-6V-2Sn alloy increased moderately with strain rate, whereas the 6Al-4V alloy evidenced a



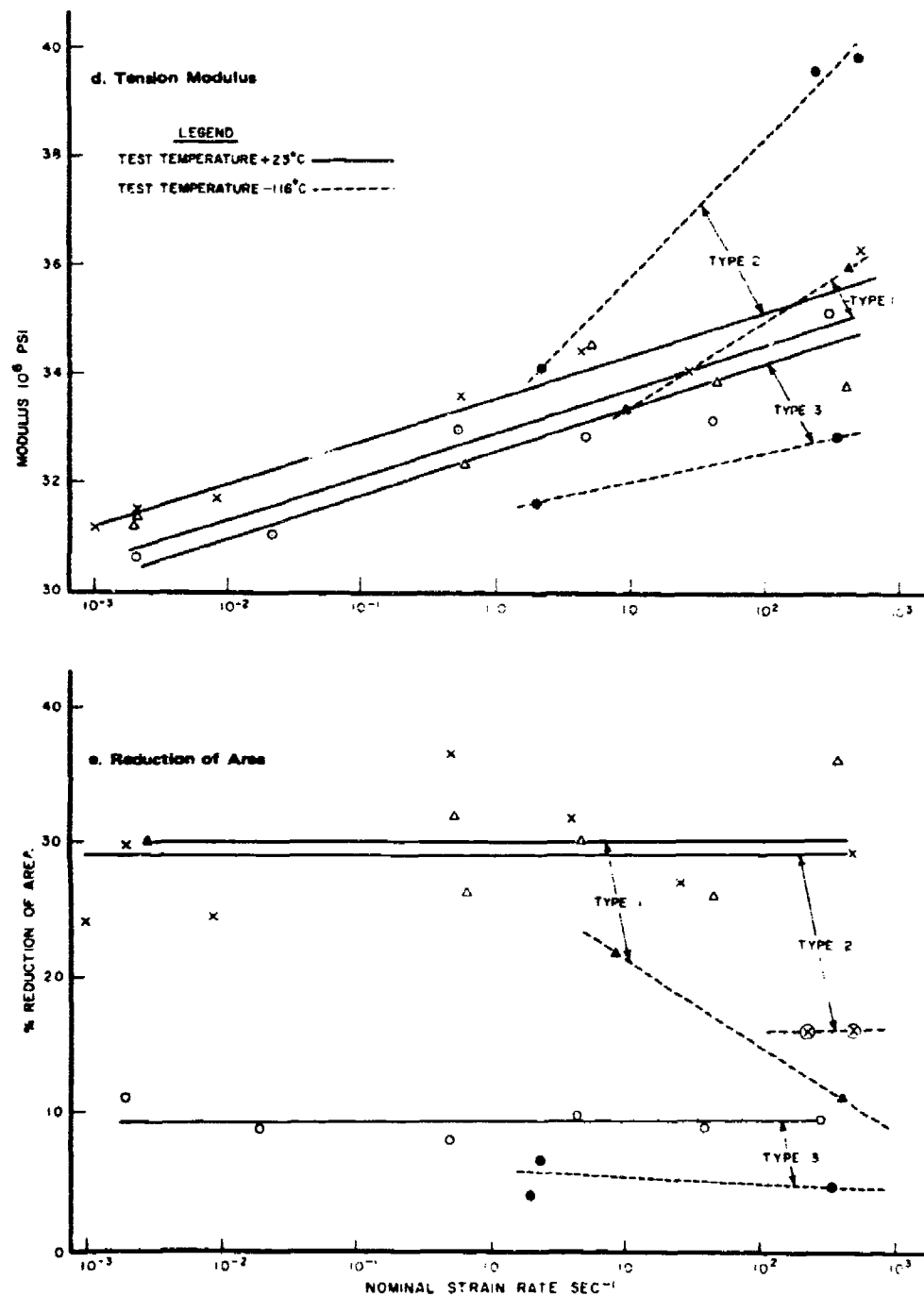


Figure 5. Relationship of mechanical properties versus strain rate for HF-1 steel

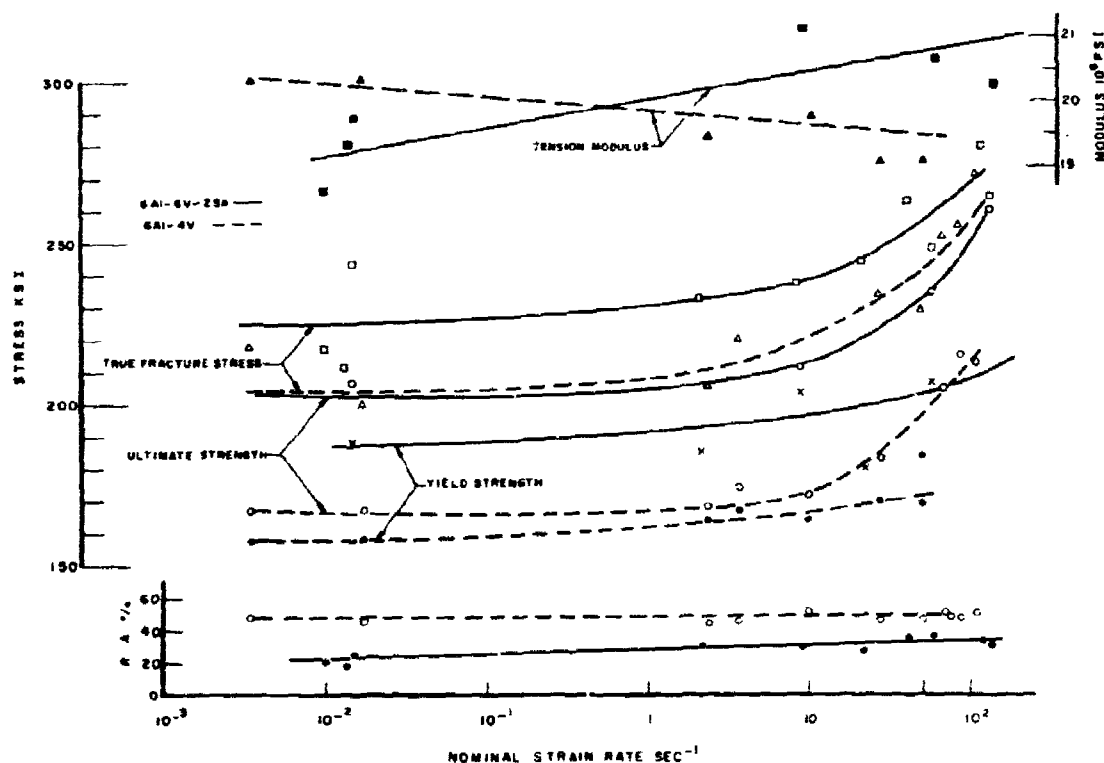


Figure 6. Mechanical properties of tested titanium alloys

moderate decline in the modulus value over the strain rate spectrum investigated. The reduction of area for the 6Al-4V alloy remained constant with strain rate, while for the 6Al-6V-2Sn alloy there was a negligible increase. Five decades of strain rate from  $4 \times 10^{-3}$  to  $1.4 \times 10^2 \text{ sec}^{-1}$  were covered in these tests.

The results on the titanium alloys are consistent with previous data reported by Austin and Steidel<sup>5</sup> for lower strength titanium alloys. These authors also observed an increase in fracture strength for cold-rolled mild steel which coincided with results obtained for the higher strength, lower ductility HF-1 alloys but contrasted with the insignificant change observed in the high-strength type 4340 and 52100 steels.

True fracture stress, ultimate tensile strength, yield strength, tension modulus, and reduction of area are plotted as a function of nominal strain rate in Figure 7 for the 8Mo-1/2Ti uranium alloy at test temperatures of -73, 23, 149, and 260 C. Tension tests were conducted at strain rates ranging from  $5.7 \times 10^{-3}$  to  $5.3 \times 10^2 \text{ sec}^{-1}$ .

5. AUSTIN, A. L., and STEIDEL, R. F., Jr. *The Tensile Properties of Some Engineering Materials at High Rates of Strain*. Proceedings of the American Society for Testing and Materials, v. 59, 1959.

As shown in Figure 7a, the fracture stress increased markedly with increasing strain rate at room temperature and -73 C. At the elevated temperatures of 149 and 260 C there was an overall slight increase in the stress value with strain rate.

It is clearly indicated in Figures 7b and 7c that both ultimate tensile strength and yield strength levels of the uranium alloy were greatly increased with increasing strain rate from subzero through the elevated temperatures tested. These mechanical property results are in excellent agreement with data reported by other investigators. Iannelli et al.<sup>6</sup> and Andersen<sup>7</sup> reported an increase of approximately 27% in the ultimate strength of U-8Mo-1/2Ti at room temperature as the strain rate progressed from  $3 \times 10^{-4} \text{ sec}^{-1}$  to  $10 \text{ sec}^{-1}$ . The data presented in Figure 7b corroborate this rate of increase within 1% at the low orders of strain rate.

The influence of strain rate on the tension modulus is depicted in Figure 7d. At all test temperatures from -73 C to 260 C the modulus increased moderately from quasi-static to approximately  $3.0 \text{ sec}^{-1}$ , the rate of increase being relatively proportional; for the higher strain rates up to  $530 \text{ sec}^{-1}$  the modulus increased markedly at temperatures from -73 C to 149 C, whereas at 260 C it was essentially neutral. It will be noted that from  $3.0 \text{ sec}^{-1}$  to  $530 \text{ sec}^{-1}$  the rate of increase of the modulus became more pronounced as the temperature decreased from 260 C to -73 C.

At the subzero temperature of -73 C, where the largest rate increase in the tension modulus occurred, an increase of approximately 94% was obtained as the strain rate increased from  $1.5 \times 10^{-2} \text{ sec}^{-1}$  to  $2.27 \times 10^2 \text{ sec}^{-1}$ . This dramatic rise in the modulus value, from  $12.0 \times 10^6 \text{ psi}$  to  $23.3 \times 10^6 \text{ psi}$ , can be attributed to a substantial change in the stress-strain behavior of the material with strain rate. Since the modulus is directly proportional to the elastic stress and inversely proportional to the strain corresponding to this stress, an appreciable change in these parameters will reflect a significant difference in the modulus level, particularly if the combined changes are cumulative, e.g., an increase in the stress value concurrent with a decrease in the strain value. Referring to Table A-4 in the Appendix, it is observed that the yield stress for the 8Mo-1/2Ti uranium alloy increased from 167 ksi to 206 ksi while the corresponding strain decreased from 0.0135 in./in. to 0.0087 in./in. These results indicate that when the stress increased 23% the corresponding strain decreased 36% with the net combined interaction of these effects contributing to an increase of approximately 93% in the tension modulus value.

Figure 7e graphically reveals the severe loss in ductility with increasing strain rate as the temperature decreased from 260 C to -73 C. At each temperature level, with the exception of 260 C where an incremental increase in ductility was noted, the loss in ductility was more pronounced at the high orders of strain rate. Figure 8 displays both the brittle and ductile type fracture modes occurring at test temperatures of -73 C and 149 C.

6. IANNELLI, A. A., and RIZZITANO, F. J. *Notched Properties of High-Strength Alloys at Various Load Rates and Temperatures*. Army Materials and Mechanics Research Center AMRA TR 66-13, July 1966 (AD647884).

7. ANDERSEN, A. G. H. *A Medium-Speed Tensile Testing Machine and Some Dynamic Data Produced Thereby*. *Journal of Applied Polymer Science*, v. 8, 1964, p. 169-196.

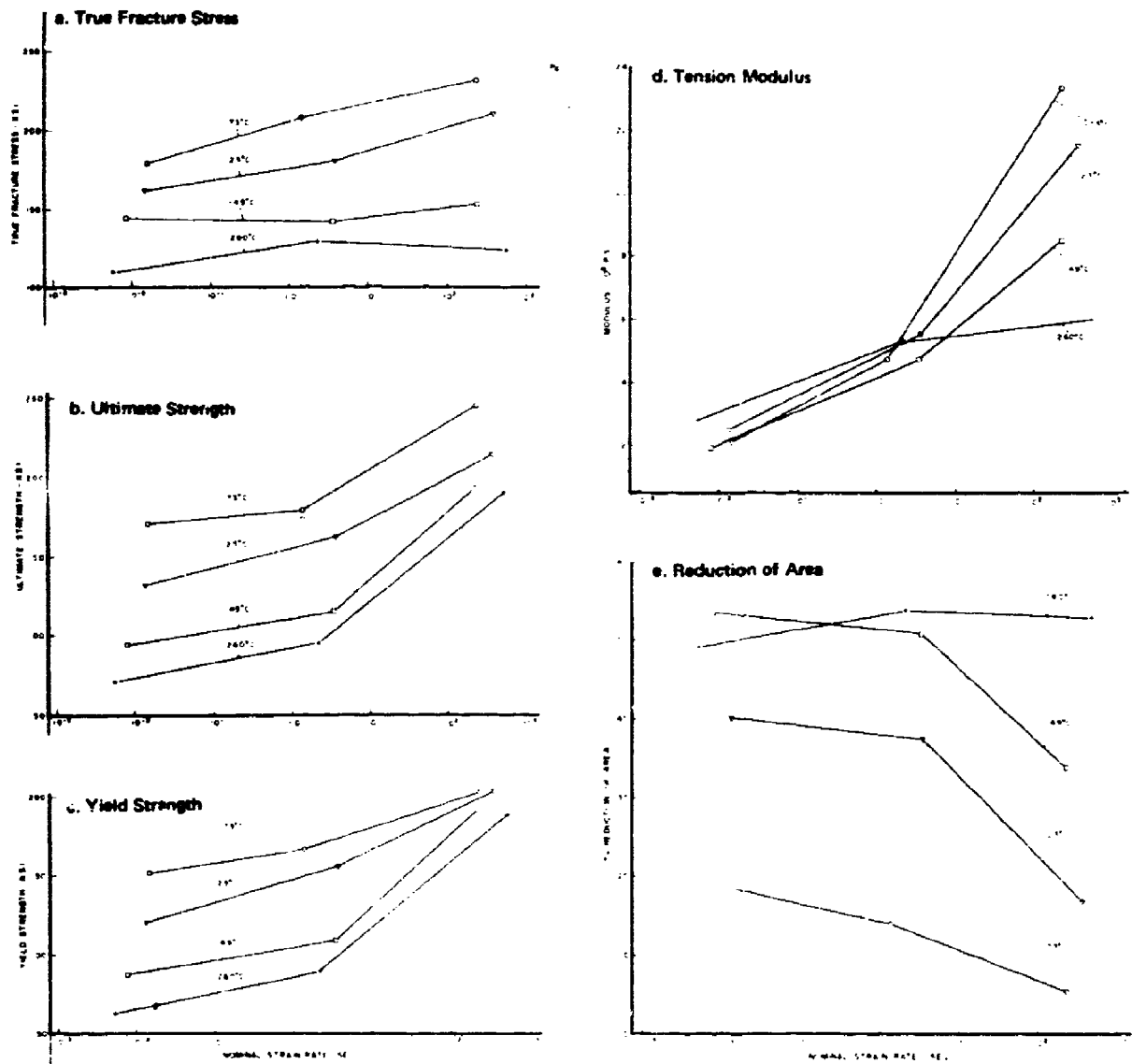


Figure 7. Relationship of mechanical properties versus strain rate for U-8Mo-1/2Ti alloy

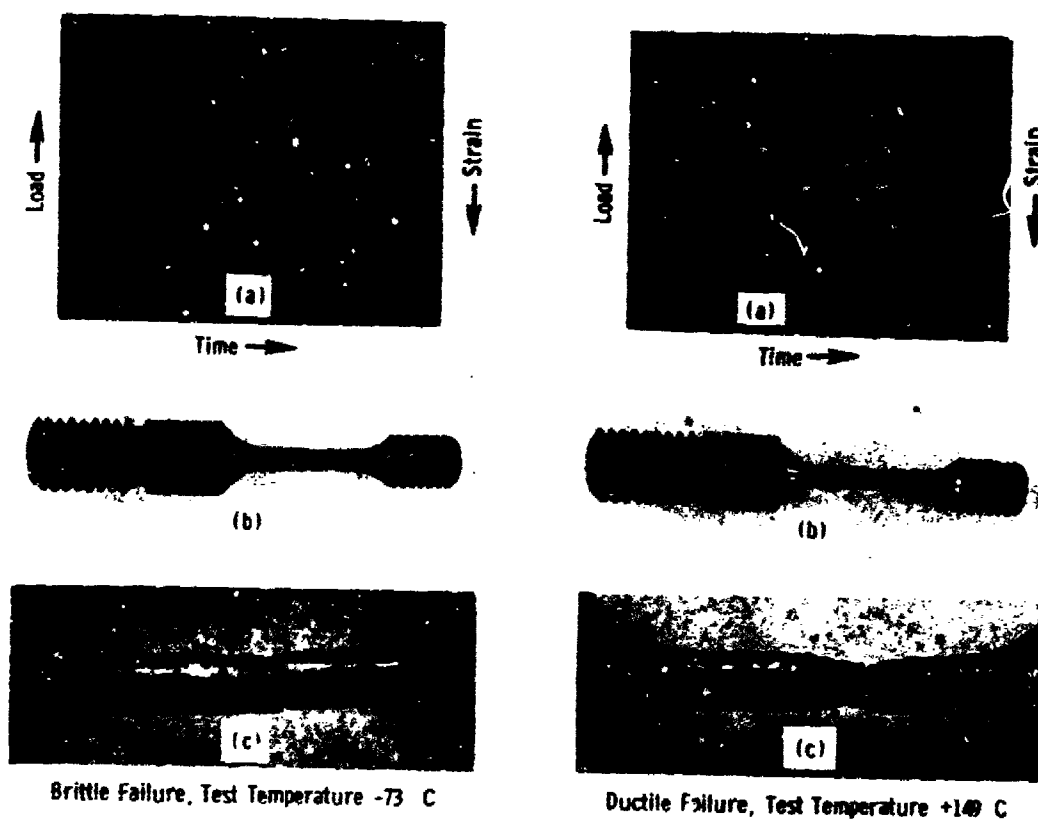


Figure 8. Typical load-time and strain-time oscillographic records of U-8Mo- $\frac{1}{2}$ Ti at elevated and subzero temperatures. (a) load-time and strain-time phenomena, (b) fractured specimen, and (c) closeup of fractured area.

In order to evaluate the relative strain rate sensitivity merits of each material under study, the cumulative differentials in mechanical property values attributed solely to strain rate variations were analyzed. Since every material was not subjected to all temperature variations, from subzero to elevated, only those temperatures that were common to all materials tested were considered as a basis for comparative evaluation. This criteria eliminated all temperatures except ambient or room temperature (23 C). Hence at ambient temperature, the sensitivity dependence of each material was determined by correlating the net differentials occurring in each of the five mechanical property parameters, i.e., true fracture stress, ultimate strength, yield strength, tension modulus, and reduction of area. The contributions of each parameter was equally weighted in arriving at the cumulative influence from which the sensitivity ratings shown in Table 4 were derived.

Examination of Table 4 indicates that of all the materials tested, U-8Mo- $\frac{1}{2}$ Ti was most sensitive to strain rate effects, being approximately twice as sensitive as the next ranking material, namely, the HF-1 steel alloy having a tempered martensitic microstructure with grain boundary network (Type 1). It is interesting to note that the S2100 steels were all least effected by strain rate variations. However, there was insufficient data on the S2100 steel to accurately assess the yield strength and tension modulus.

Since the uranium alloy was subjected to subzero as well as elevated temperature environments, the effect of temperature on the strain rate sensitivity of this material could then be ascertained. The cumulative sensitivity influence at each temperature was determined and compared with the room temperature (23 C) results as shown in Table 5. It will be noted from Table 5 that, in general, as the test temperature decreased the effect of temperature on the strain rate sensitivity decreased with a very slight change (5.7%) occurring from +149 C to +23 C. As the temperature increased from +23 C to +260 C the strain rate sensitivity influence of this uranium alloy increased by approximately 80%, whereas from +23 C to -73 C there was a decrease of approximately 50% in the sensitivity indicator.

Table 4. STRAIN RATE EVALUATION OF VARIOUS BRITTLE AND TOUGH MATERIALS  
IN DESCENDING ORDER OF SENSITIVITY DETERMINED AT AMBIENT TEMPERATURE (-23 C)

Test Material	Sensitivity Dependence of Each Parameter for Maximum Range of Strain Rate Data - Net Differential ( )					Sensitivity Indicator Cumulative Sensitivity Influence ( )	Sensitivity Rating
	True Fract. Stress	Ult. Str.	Yield Str.	Tension Modulus	R.A.		
U-8Mo-1/2Ti	37.7	67.7	71.9	99.2	70.6	347.1	A
HF-1 (Type 1)	6.4	22.4	80.6	28.8	37.7	175.9	B
Ti-6Al-6V-2Sn	32.1	26.1	21.3	8.6	76.3	164.4	C
HF-1 (Type 3)	21.3	27.2	58.6	14.4	16.2	137.7	D
HF-1 (Type 2)	37.6	24.3	26.8	16.0	19.9	124.6	E
4340 (Q&T)	10.2	16.9	22.3	25.3	3.6	78.3	F
Ti-6Al-4V	24.3	28.6	7.0	6.4	5.6	71.9	G
52100-2 (IQ&T)	7.3	9.4	18.4	1.6	14.5	50.2	H
52100-3 (Norm&T)	2.4	3.9	8.9	0.3	27.9	43.4	I
52100-1 (IQ&T)	0.5	7.9	-	-	27.9	36.3	*

\*Not rated due to unavailability of related data

Table 5. EFFECT OF TEMPERATURE ON STRAIN RATE SENSITIVITY  
OF GAMMA-STABILIZED U-8Mo-1/2Ti

Test Temp. (Deg C)	Sensitivity Influence of Each Parameter for Maximum Range of Strain Rate Data - Net Differential ( )					Cumulative Sensitivity Influence ( )	Temp. Effect - Change in Sensitivity Influence ( ) Relative to Ambient Temp. (23 C)
	True Fract. Stress	Ult. Str.	Yield Str.	Tension Modulus	R.A.		
+ 23	37.7	67.7	71.9	99.2	70.6	347.1	-
- 73	41.7	44.1	36.0	94.2	79.5	295.5	-51.6
+149	14.5	110.9	120.5	66.7	40.2	352.8	+ 5.7
+260	19.2	175.4	196.9	16.4	17.5	425.4	+78.3

For the HF-1 steel in the three heat-treated conditions the effect of the subzero temperature (-116 C) on the strain rate sensitivity characteristics was investigated. There was sufficient data to effect a comparison of the cumulative sensitivity influence at -116 C with that obtained at +23 C for Types 1 and 3 only. Examination of Table 6 reveals that the strain rate sensitivity decreased for Types 1 and 3 as the temperature decreased from +23 C to -116 C, the temperature effect being greater for Type 3 by a factor of approximately 1.9. In assessing the overall strain rate influence at -116 C, the results indicate that Type 3 was least affected by strain rate variations, its sensitivity being significantly less (62%) than the Type 1 alloy.

From an analysis of the test data, a methodology was evolved to crystallize the extent of temperature effects, at constant strain rate, on the mechanical property results of both the gamma-stabilized U-8Mo-1/2Ti and the HF-1 steel in the three heat-treated conditions. To implement this concept, the net changes occurring in each mechanical property parameter relative to its ambient temperature performance was initially determined. By placing equal emphasis on each value thus obtained, it was then possible to correlate the resultant cumulative differential which would be considered indicative of the comprehensive influence of the temperature contribution. Each entry contained in the cumulative indicator resulted from the behavior at the two strain rates formed at the boundaries of the spectrum evaluated.

For the gamma-stabilized uranium alloy under quasi-static loading conditions, it will be noted from Table 7 that the temperature influence remained fairly constant as the temperature either increased from +23 C to +149 C or decreased to -73 C but a moderate change (38%) was realized when the temperature increased to +260 C. In comparison with the low-order strain rate results, the temperature effects, under dynamic loading rates, were much more pronounced at the elevated test conditions, whereas a relatively modest change occurred at the subzero temperature.

In the case of the HF-1 steel at low-order strain rates the temperature influence on the mechanical property results of Type 3 material was approximately 64% greater than that of Type 1; Type 2 was excluded from this analysis due to insufficient data points. The temperature interaction resulting at high-order strain rate conditions, even though the levels of susceptibility were higher than those attained at low-order strain rates (Table 8), was quite comparable for all three types of HF-1 steel; a maximum difference of only 17% occurred and that was between Types 1 and 3. At high-order strain rate conditions the three types of HF-1 steel can be ranked in the following descending order of susceptibility to the subzero temperature change from +23 C to -116 C: Types 1, 3, and 2.

For the HF-1 steel alloy having the tempered martensite microstructure with grain boundary network (Type 1), the temperature effects at high-order strain rates were approximately twice (1.94) that occurring at low-order strain rates. However, temperature effects on the HF-1 alloy in the isothermally transformed to coarse pearlite microstructure (Type 3) were relatively independent of strain rate wherein a negligible difference of 5% was obtained at the extremities of the strain rate range examined.

Table 6. EFFECT OF TEMPERATURE ON STRAIN RATE SENSITIVITY OF HF-1 STEEL IN THREE HEAT-TREATED CONDITIONS

Sensitivity Influence of Each Parameter for Maximum Range of Strain Rate Data - Net Differential (%)								
Material	Test Temp. (Deg C)	True Fract. Stress	Ult. Str.	Yield Str.	Tension Modulus	R.A.	Cumulative Sensitivity Influencer ( )	Temp. Effect - Change in Sensitivity Influence ( ) Relative to Ambient Temp. (23 C)
Type 1	23	6.4	22.4	80.6	28.8	37.7	175.5	-
Type 1	-116	15.5	28.4	14.7	7.8	43.7	110.1	-37.4
Type 2	23	37.6	24.3	26.8	16.0	19.9	124.6	-
Type 2	-116	-	1.0	17.1	16.7	-	"	-
Type 3	23	21.3	27.2	58.6	14.4	16.2	137.7	-
Type 3	-116	0.9	0.3	23.9	3.8	13.2	42.1	-69.4

\*Not tabulated due to insufficient data

Table 7. EFFECT OF TEMPERATURE ON MECHANICAL PROPERTY RESULTS OF GAMMA-STABILIZED U-Mo-1/2Ti UNDER QUASI-STATIC AND DYNAMIC LOADING CONDITIONS

Net Change (%) in Each Parameter Relative to Ambient Temp. (23 C) at Strain Rates $R_a^*$ and $R_b^*$ (Sec <sup>-1</sup> )													
Test Temp. (Deg C)	True Fract. Stress		Ult. Str.		Yield Str.		Tension Modulus		R.A.		Cumulative Temp. Effect Differential ( )		Comparison of Temp. Effects at High- and Low-Order Strain Rates $R_b/R_a$
	$R_a$	$R_b$	$R_a$	$R_b$	$R_a$	$R_b$	$R_a$	$R_b$	$R_a$	$R_b$	$R_a$	$R_b$	
- 73	9.1	12.3	30.8	12.4	19.3	1.9	1.6	4.1	37.1	56.1	102.6	86.6	0.85
+149	10.4	25.5	29.2	11.0	27.3	6.7	4.1	19.8	28.0	160.2	99.0	223.2	2.25
+260	32.5	41.5	46.9	12.8	47.1	8.7	4.9	38.7	10.5	341.5	141.9	443.2	3.12

\* $0.006 \leq R_a \leq 0.015$

+ $2.27 \times 10^2 \leq R_b \leq 5.31 \times 10^2$

Table 8. EFFECT OF SUBZERO TEMPERATURE (-116 C) ON MECHANICAL PROPERTY RESULTS OF HF-1 STEEL IN THREE HEAT-TREATED CONDITIONS AT LOW- AND HIGH-ORDER STRAIN RATES

Net Change (%) in Each Parameter Relative To Ambient Temp. (23 C) at Strain Rates $R_a^*$ and $R_b^*$ (Sec <sup>-1</sup> )													
Material	True Fract. Stress		Ult. Str.		Yield Str.		Tension Modulus		R.A.		Temp. Index Cumulative Differential ( )		Comparison of Temp. Effects at High- and Low-Order Strain Rates $R_b/R_a$
	$R_a$	$R_b$	$R_a$	$R_b$	$R_a$	$R_b$	$R_a$	$R_b$	$R_a$	$R_b$	$R_a$	$R_b$	
Type 1	5.9	15.5	5.2	26.4	11.6	5.4	3.5	15.9	28.6	39.4	52.8	102.6	1.94
Type 2	-	15.1	4.3	5.2	9.0	9.6	0.9	9.9	-	45.7	*	85.5	*
Type 3	13.4	14.1	7.7	12.2	0.6	4.8	3.7	6.3	60.8	53.8	86.6	91.2	1.05

\*Not determined due to insufficient data

+ $2.04 \leq R_a \leq 9.19$

+ $2.86 \times 10^2 \leq R_b \leq 5.32 \times 10^2$

True stress-true strain curves as a function of strain rate were plotted in logarithmic coordinates for each material tested to present a better view of the strain hardening phenomenon. Since the relationships thus established could be analytically expressed in the form of  $\sigma = K\epsilon^n$ , the strain hardening exponent  $n$  is directly determined from the slope of these curves. Changes in the slopes of the curves, occurring at various strain rates, could then be interpreted in terms of the development of hardening or softening processes.

Room temperature true stress-true strain curves at various strain rates for the 4340 and 52100 steels as well as the 6Al-4V and 6Al-6V-2Sn titanium alloys are shown in Figure 9. The 4340 (Q&T) steel alloy and the titanium alloys all exhibited a decrease in strain hardening with increased strain rate. The 6Al-6V-2Sn and 6Al-4V titanium alloys showed a significant general increase in flow stress but no apparent change in fracture behavior. For the 52100 steels, in both the grain boundary embrittled low temper and normalized conditions, there was no change in strain hardening with increasing strain rate; however, for the grain boundary embrittled high temper condition, strain hardening increased with increasing strain rate.

The results on strain hardening for the 6Al-4V titanium alloy are consistent with a previous investigation by Johnson et al.<sup>8</sup> who observed a decrease in strain hardening at high strain rates up to  $8000 \text{ sec}^{-1}$ . These investigators did, however, observe an increase in the strain hardening slope at high strain rates for Type 304 stainless steel, Armco iron, and unalloyed aluminum.

The true stress-true strain characteristics at room temperature for the three types of HF-1 steel at various strain rates are shown in Figure 10. Types 2 and 3 showed a fairly significant increase in flow stress with increasing strain rate but with no apparent change in fracture behavior. Strain hardening for Type 1 material showed a pronounced decrease with increased strain rate, whereas with Types 2 and 3 the decrease in slope was insignificant.

Figure 11 displays the true stress-true strain curves at various strain rates of HF-1 steel for the test temperature of  $-116^\circ\text{C}$ . The strain hardening index for the three steel alloys decreased significantly with increasing strain rate, the change in slope becoming increasingly greater when progressing from the conventional tempered martensite (Type 1) through the tempered martensite with grain boundary network (Type 2) to the isothermally transformed coarse pearlitic (Type 3) microstructures. The accelerated softening mechanism was evidenced from examination of the net percentage changes developed in the slope of the true stress-true strain curves, i.e., 22.2% for Type 1; 37.1% with Type 2; and 43.4% by Type 3.

The true stress-true strain behavior for the gamma-stabilized 8Mo-1/2Ti uranium alloy at various strain rates and test temperatures is presented in Figure 12. With the exception of subzero temperature of  $-73^\circ\text{C}$ , where an increase in the strain hardening slope occurred with increasing strain rate, strain hardening in general decreased with increasing strain rate as the temperature increased from  $23^\circ\text{C}$  to  $260^\circ\text{C}$ .

8. JOHNSON, P. C., STEIN, B. A., and DAVIS, R. S. *Measurement of Dynamic Plastic Flow Properties Under Uniform Stress*. ASTM STP 336, 1963, p. 195-205.

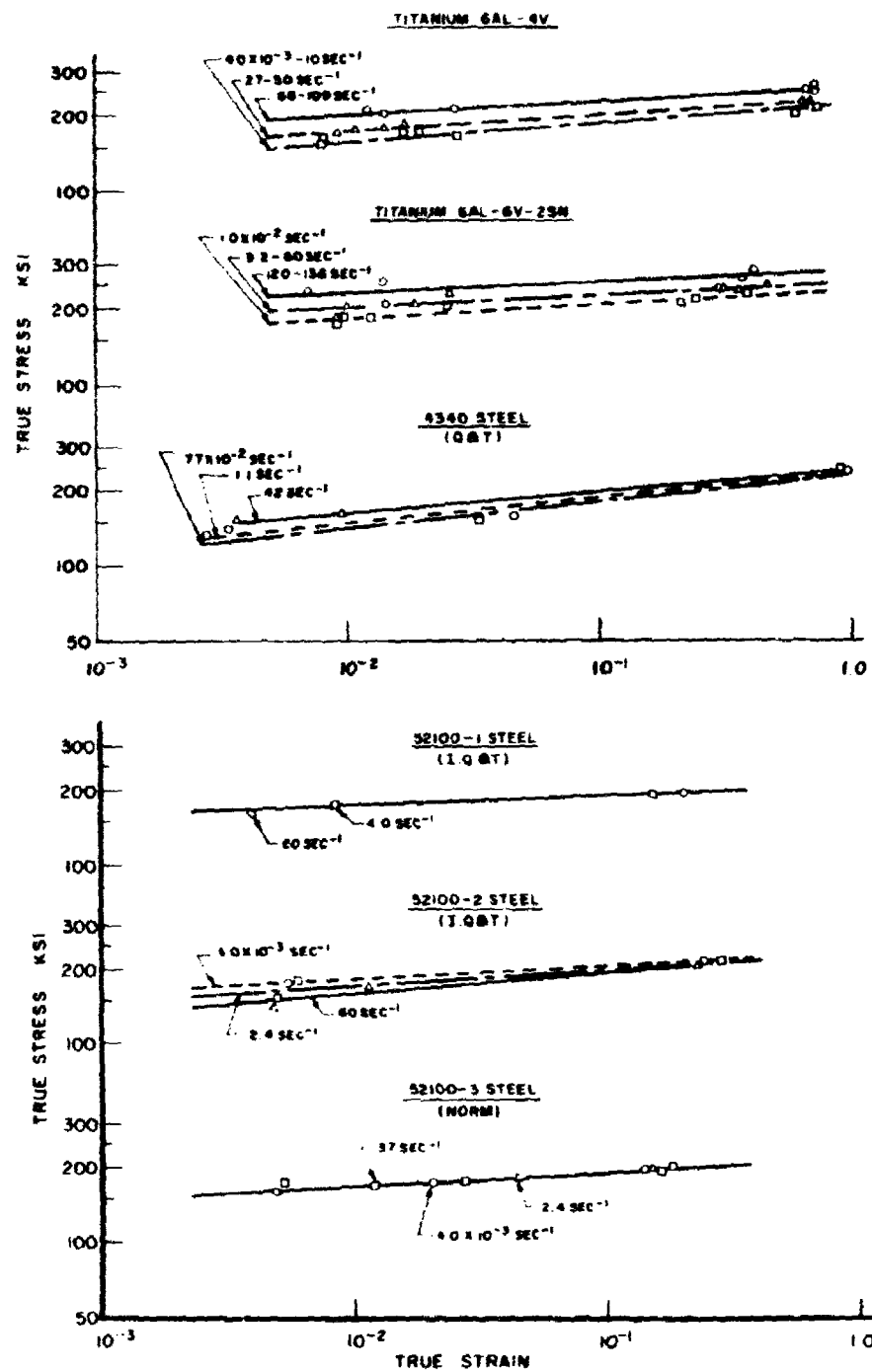


Figure 9. True stress-true strain results for titanium alloys and 4340 and 53100 steels

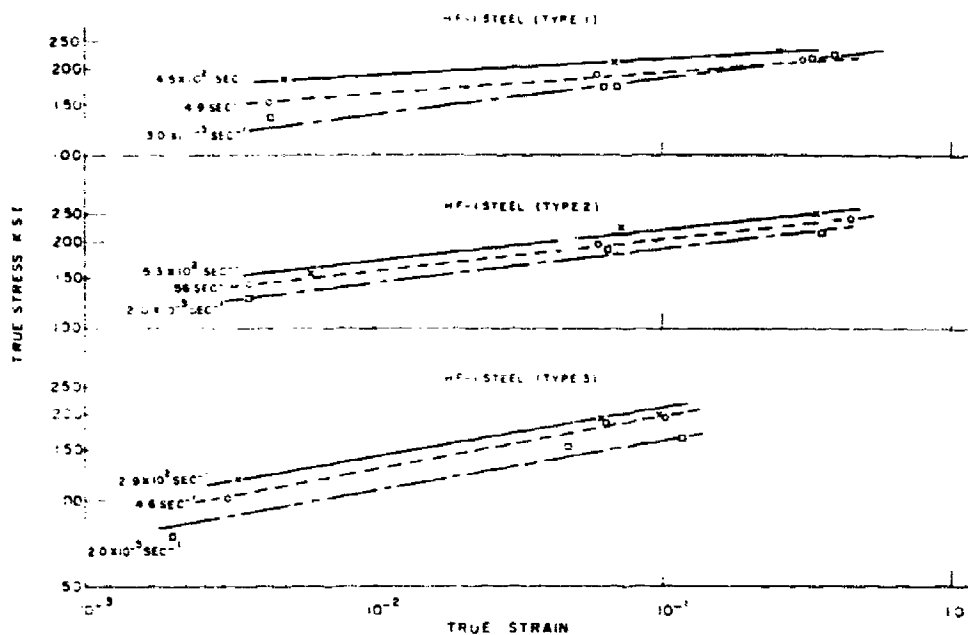


Figure 10. True stress-true strain results for HF-1 steel (test temperature +23 C)

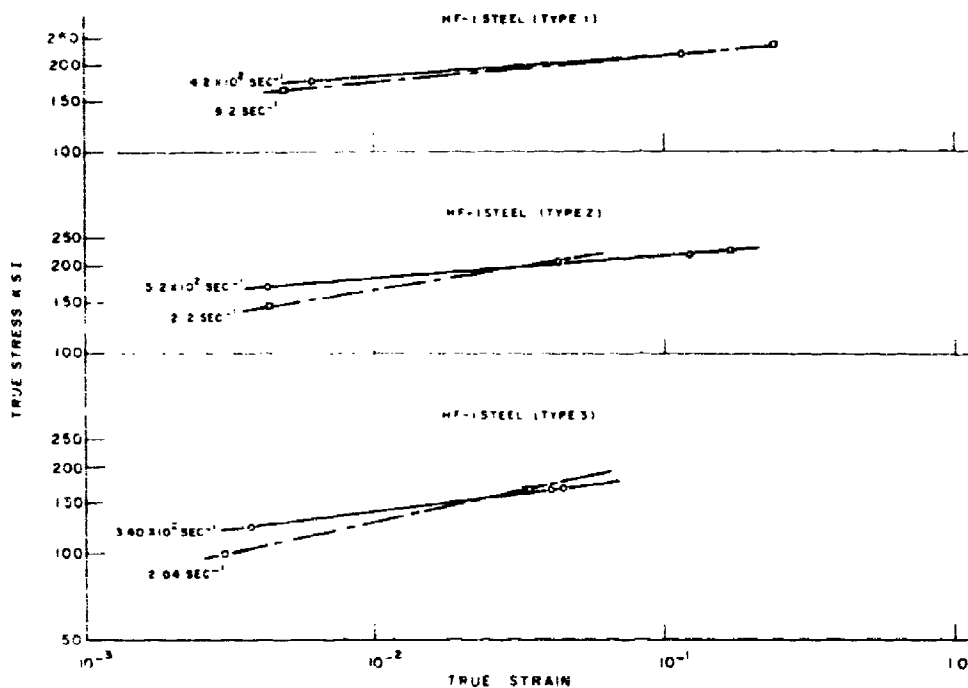


Figure 11. True stress-true strain results for HF-1 steel (test temperature -116 C)

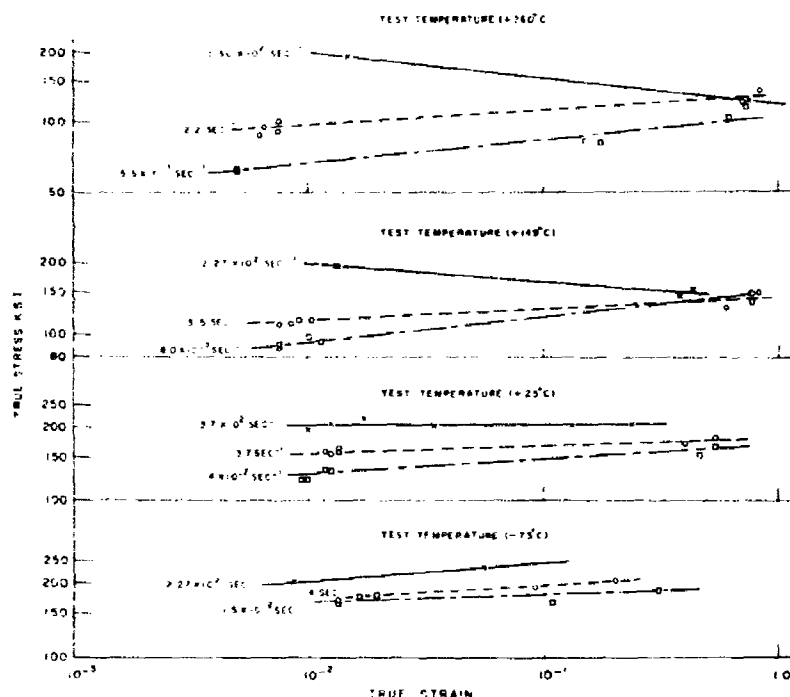


Figure 12. True stress-true strain results for 8Mo- $\frac{1}{2}$ Ti uranium alloy

In an attempt to assess the strain hardening characteristics of the various materials tested, the strain hardening index  $n$  was first graphically obtained from the true stress-true strain curves plotted in Figures 9 to 12. Thus the strain hardening indices were directly determined from the slopes of these curves for each material grouping at all test temperatures and the results are presented in Table 9.

Similar to the procedure set up for determining the strain rate sensitivity dependence of each material, since the only temperature common to all materials was ambient or room temperature (+23 C), the strain hardening behavior at ambient temperature was selected as the criterion for comparable evaluation. Thereupon the strain hardening index for each material was quantified at three levels of strain rate performance, representing low-, intermediate-, and high-order magnitudes (Table 10) from which the net changes (%) in the strain hardening index was computed over the maximum span of strain rate data available.

As a result of this computation, each material was rated in descending order of strain hardening influence as shown in Table 11. The 8Mo- $\frac{1}{2}$ Ti uranium alloy was the most sensitive to strain hardening behavior, registering a net change of -89.6%, the negative sign indicating that the strain hardening slope decreased with strain rate, thereby signalling the development of a softening process. The same phenomenon, the incipency of a softening process, was germane to all the brittle and tough materials evaluated with the exception of the 52100-2 (IQ&T) alloy which exhibited an increase in slope with strain rate indicating the development of a strain hardening mechanism. It is interesting to note the extreme

Table 9. STRAIN HARDENING REACTION OF MATERIALS AT VARIOUS TEST TEMPERATURES  
FOR EACH MATERIAL GROUPING IN DESCENDING ORDER OF SLOPE VALUES

Material	Strain Rate (Sec <sup>-1</sup> )	Test Temp. (Deg C)	Strain Hardening Index (n)
U-8Mo-1/2Ti	$5.30 \times 10^2$	+260	-0.1095
	$8.0 \times 10^{-3}$	+149	+0.1051
	$5.5 \times 10^{-1}$	+260	.0992
	$2.27 \times 10^2$	- 73	.0802
	1.4	- 73	.0758
	$2.27 \times 10^2$	+149	-0.0729
	$1.4 \times 10^{-2}$	+ 23	+0.0699
	2.2	+260	.0670
	3.5	+149	.0510
	3.7	+ 23	.0378
	$1.5 \times 10^{-2}$	- 73	.0262
	$3.7 \times 10^2$	+ 23	.0073
4340	$0.77 \times 10^{-2}$	Ambient	+0.1110
	1.1	Ambient	.1080
	42	Ambient	.0802
Ti-6Al-6V-2Sn	$1.0 \times 10^{-2}$	Ambient	+0.0568
	9.2 to 60	Ambient	.0481
	120 to 136	Ambient	.0452
Ti-6Al-4V	$4.0 \times 10^{-3}$	Ambient	+0.0773
	27 to 50	Ambient	.0670
	68 to 109	Ambient	.0553
52100-1	4.0 to 60.0	Ambient	+0.0349
52100-2	60	Ambient	+0.0875
	2.4	Ambient	.0670
	$4.0 \times 10^{-3}$	Ambient	.0524
52100-3	$4.0 \times 10^{-3}$	Ambient	+0.0568
	2.4	Ambient	.0568
	37	Ambient	.0568
HF-1 (Type 1)	$3.0 \times 10^{-3}$	+ 23	+0.1228
	9.2	-116	.0904
	49	+ 23	.0729
	$4.2 \times 10^2$	-116	.0699
	$4.5 \times 10^2$	+ 23	.0553
HF-1 (Type 2)	2.2	-116	+0.1554
	$2.0 \times 10^{-3}$	+ 23	.1184
	0.56	+ 23	.1095
	$5.3 \times 10^{-3}$	+ 23	.1095
	$5.2 \times 10^2$	-116	.0978
HF-1 (Type 3)	2.04	-116	+0.2156
	$2.0 \times 10^{-3}$	+ 23	.1778
	4.6	+ 23	.1778
	$2.9 \times 10^2$	+ 23	.1659
	$3.40 \times 10^2$	-116	.1228

Table 10. RELATIVE STRAIN HARDENING BEHAVIOR OF VARIOUS BRITTLE AND TOUGH MATERIALS DETERMINED FOR THREE LEVELS OF STRAIN RATE AT AMBIENT TEMPERATURE (~23 C)

Levels of Strain Rate	Strain Rate (Sec <sup>-1</sup> )	Strain Hardening Index (n)	Test Material
High	$2.9 \times 10^2$	0.1659	HF-1 (Type 3)
$1.1 \times 10^2$ to $5.3 \times 10^2$ sec <sup>-1</sup>	$5.3 \times 10^2$	.1095	HF-1 (Type 2)
	$4.5 \times 10^2$	.0553	HF-1 (Type 1)
	$1.1 \times 10^2$	.0553	Ti-6Al-4V
	$1.4 \times 10^2$	.0452	Ti-6Al-6V-2Sn
	$3.7 \times 10^2$	.0073	U-8Mo-1/2Ti
Intermediate 2.4 to 60 sec <sup>-1</sup>	4.6	0.1778	HF-1 (Type 3)
	60	.0875	52100-2
	42	.0802	4340
	49	.0729	HF-1 (Type 1)
	9.2 to 60	.0568	Ti-6Al-6V-2Sn
	2.4 to 37	.0568	52100-3
	27 to 50	.0553	Ti-6Al-4V
	3.7	.0378	U-8Mo-1/2Ti
	4.0 to 60	.0349	52100-1
Low $2.0 \times 10^{-3}$ to $1.4 \times 10^{-2}$ sec <sup>-1</sup>	$2.0 \times 10^{-3}$	0.1778	HF-1 (Type 3)
	$3.0 \times 10^{-3}$	.1228	HF-1 (Type 1)
	$2.0 \times 10^{-3}$	.1184	HF-1 (Type 2)
	$0.77 \times 10^{-2}$	.1110	4340
	$4.0 \times 10^{-3}$	.0773	Ti-6Al-4V
	$1.4 \times 10^{-2}$	.0699	U-8Mo-1/2Ti
	$1.0 \times 10^{-2}$	.0568	Ti-6Al-6V-2Sn
	$4.0 \times 10^{-3}$	.0568	52100-3
	$4.0 \times 10^{-3}$	.0524	52100-2

range in the strain hardening susceptibility developed by the 52100 steels; the alloy in the grain boundary embrittled high temper condition (IQ&T) was ranked second, whereas the alloy in the normalized condition (Norm&T), which remained neutral to strain hardening effects, was ranked last.

In view of the fact that mechanical tests were performed with the U-8Mo-1/2Ti alloy at various temperatures, ranging from subzero to elevated, the effects of temperature on the strain hardening characteristics of the material could be studied in detail. The strain hardening index versus strain rate as a function of temperature was initially plotted in semi-logarithmic coordinates to graphically demonstrate the influence of temperature on the strain hardening behavior. By noting the slopes of the curves developed in Figure 13a and the rate of change of these slopes relative to ambient temperature (+23 C) as given in Table 12, the results could then be interpreted in terms of the influence the various temperatures exerted on the development of a hardening or softening process.

From Figure 13a, it is evident that at +23 C the strain hardening index for the uranium alloy behaved linearly throughout the entire strain rate range, whereas at elevated and subzero temperatures the data suggested that a dual sloped curve would more accurately define the strain hardening reaction occurring under low-order and high-magnitude strain rate conditions. Since the transition point of

Table 11. EVALUATION OF STRAIN HARDENING CHARACTERISTICS OF VARIOUS BRITTLE AND TOUGH MATERIALS IN DESCENDING ORDER OF INFLUENCE DETERMINED AT AMBIENT TEMPERATURE (+23 C)

Test Material	Strain Hardening Index for Three Levels (L,I,H)* of Strain Rate			Net Change in Strain Hardening Index, Percent† (X*-n <sub>1</sub> /n <sub>1</sub> ) × 100	Influence Rating
	n <sub>1</sub>	n <sub>2</sub>	n <sub>3</sub>		
U-8Mo-1/2Ti	0.0699	0.0378	0.0073	-89.6	A
52100-2 (IQ&T)	.0524	.0875	-	+67.0	B
HF-1 (Type 1)	.1228	.0729	.0553	-55.0	C
Ti-6Al-4V	.0773	.0553	.0553	-28.4	D
4340 (Q&T)	.1110	.0802	-	-27.7	E
Ti-6Al-6V-2Sn	.0568	.0568	.0452	-20.4	F
HF-1 (Type 2)	.1184	-	.1095	- 7.5	G
HF-1 (Type 3)	.1778	.1778	.1659	- 6.7	H
52100-3 (Norm&T)	.0568	.0568	-	0	I
52100-1 (IQ&T)	-	.0349	-	-	†

\*L - Low values of strain rate ( $2.0 \times 10^{-3}$  to  $1.4 \times 10^2 \text{ sec}^{-1}$ ).

I - Intermediate levels of strain rate (2.4 to  $60 \text{ sec}^{-1}$ ).

H - High magnitudes of strain rate ( $1.1 \times 10^2$  to  $5.3 \times 10^2 \text{ sec}^{-1}$ ).

X - Strain hardening index, n<sub>2</sub> or n<sub>3</sub>, selected to yield maximum range of extant strain rate data.

†Negative numbers are indicative of softening process whereas positive numbers relate the strain hardening characteristic.

‡Not rated due to insufficient comparable data.

these discontinuous curves occurred at a strain rate of approximately  $4.0 \text{ sec}^{-1}$ , equal consideration was given to the influence generated above and below this value.

It can be hypothesized from the data, as presented in Table 12, that under the influence of the subzero and elevated temperature environment, at low-order strain rate conditions, a strain hardening mechanism predominated, whereas at high magnitudes of strain rate the development of a softening process prevailed. As a result of the elevated and subzero temperature input, under low-order strain rate conditions, the following significant changes in the strain hardening characteristics of the uranium alloy relative to ambient temperature (+23 C) was noted: (1) an approximate threefold increase in strain hardening was incurred at the subzero temperature of -73 C; (2) a substantial decrease in strain hardening of the order of 50% was realized at the elevated temperature of +149 C; and (3) a relatively insignificant change (7.6%) occurred at +260 C. At high-magnitude strain rates, irrespective of the fact that the maximum sensitivity levels encountered were significantly greater than that achieved at low-order strain rates, the susceptibility of the strain hardening behavior to temperature variations was quite comparable at both elevated temperatures; in contrast, at the subzero temperature of -73 C, the influence of temperature was much less severe (by a factor of approximately 1/3) than that determined at low-order strain rates.

Table 12. EFFECT OF TEMPERATURE ON STRAIN HARDENING BEHAVIOR  
OF GAMMA-STABILIZED U-8Mo-1/2Ti

Test Temp. (Deg C)	Strain Hardening Index Slope $m$ , at Strain Rate, $R$ , (Sec <sup>-1</sup> )		Change in Strain Hard- ening Index Slope $\Delta m = m_1 - m_0$ at Strain Rate, $R$ , (Sec <sup>-1</sup> )		Rate of Change of Strain Hardening Index Slope, Per- cent,** Relative to Ambient Temp. (23 C) at Strain Rate, $R$ , (Sec <sup>-1</sup> ) ( $\Delta m/m_0 \times 100$ )	
	$R_a^+$	$R_b^+$	$R_a^+$	$R_b^+$	$R_a^+$	$R_b^+$
+ 23 ( $T_0$ )	-0.1346	-0.1346	-	-	-	-
- 73 ( $T_1$ )	+0.2705	+0.0306	+0.4051	+0.1652	-301	-123
+149 ( $T_2$ )	-0.2035	-0.6787	-0.0689	-0.5441	+ 51	+404
+260 ( $T_3$ )	-0.1243	-0.7468	+0.0103	-0.6122	-7.6	+455

\* $m_1$  = corresponding slope at temperature,  $T_1$ ,  $T_2$ ,  $T_3$

$m_0$  = slope at temperature,  $T_0 = -0.1346$

$-5.5 \times 10^{-3} \leq R_a \leq 3.7$

$\pm 3.7 > R_b \leq 5.2 \times 10^2$

\*\*Negative percent values indicate the required change in polarity of the  
reference slope at 23 C ( $T_0$ )

Since the uniaxial tension tests performed with the HF-1 steel in the three heat-treated conditions were conducted at +23 C as well as -116 C over the same strain rate spectrum, the influence of the subzero temperature on the strain hardening phenomenon of this alloy relative to ambient temperature (+23 C) could be thoroughly analyzed. By plotting, on semi-logarithmic axes, the strain hardening index against strain rate as a function of temperature, it was apparent from Figure 13b that the relationship between the strain hardening characteristic and strain rate was essentially linear for all three types of HF-1 at both subzero (-116 C) and ambient (+23 C) temperatures. Moreover, Figure 13b illustrates graphically the negligible temperature effects on the strain hardening behavior of Type 1 material as well as the dramatic sensitivity exhibited by Types 2 and 3 to the temperature influence. Figure 13b also exposes the development of a softening process for all three types of HF-1 steel when the temperature was held constant at either +23 C or -116 C; however, the severity of the resulting process reacted anomalously for each type with temperature, i.e., at +23 C, the HF-1 steel in the three heat-treated conditions was ranked in the following descending order of sensitivity: Types 1, 2, and 3, whereas at -116 C the ranking order was reversed. On the other hand, the degree of severity for the relative ranking positions was on the average approximately 11 times as great at -116 C than at +23 C.

Referring to Figure 13b, since the slopes of the strain hardening index curves obtained at test temperatures of +23 C and -116 C were essentially parallel for the HF-1 steel alloy having the tempered martensite microstructure with grain boundary network (Type 1), it can be postulated that the temperature influence on the strain hardening characteristic of this alloy could well be ignored. The rate of change of the strain hardening index slope for Type 1, referenced in Table 13, was indeed small enough (3.6%) to be virtually discounted as a contributing factor. The HF-1 alloy in the isothermally transformed to coarse pearlitic microstructure (Type 3) was extremely sensitive to the subzero (-116 C) temperature influence, wherein the strain hardening characteristic decreased by a phenomenal factor of

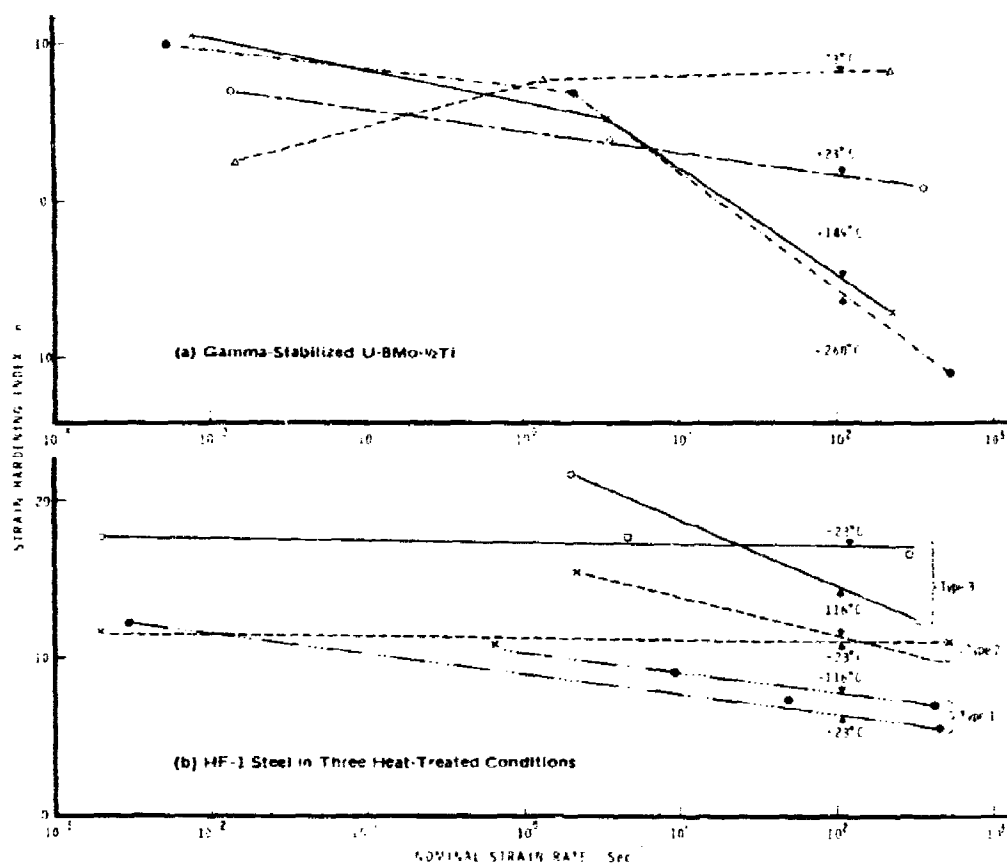


Figure 13. Influence of temperature on strain-hardening behavior

Table 13. EFFECT OF SUBZERO TEMPERATURE (-116 C) ON STRAIN HARDENING BEHAVIOR OF HF-1 STEEL IN THREE HEAT-TREATED CONDITIONS

Material	Strain Hardening Index Slope $m$ , at Temp., T		Change in Strain Hardening Index Slope, $\Delta m^* = m_1 - m_2$	Rate of Change of Strain Hardening Index Slope (%) Relative to Ambient Temp. (23 C), $(\Delta m/m) \times 100$
	23 C $m_2$	-116 C $m_1$		
Type 1	-0.1228	-0.1272	-0.0044	3.6
Type 2	-0.0160	-0.2385	-0.2225	1391.
Type 3	-0.0087	-0.4176	-0.4089	4700.

\*Slopes determined in the strain rate range covering  $2.0 \times 10^{-3}$  to  $5.3 \times 10^{-2} \text{ sec}^{-1}$

47. Type 2, the alloy having the conventional tempered martensitic microstructure, was highly susceptible to low temperature effects yielding a substantial strain hardening attenuation factor of approximately 14, irrespective of the fact that it was 3.4 times less sensitive than Type 3.

## CONCLUSIONS

The influence of strain rate on the mechanical properties of brittle and tough materials tested at room temperature covering the strain rate spectrum from  $10^{-3}$  to  $5.3 \times 10^2 \text{ sec}^{-1}$  is summarized as follows:

1. The gamma-stabilized 8Mo-1/2Ti uranium alloy was most sensitive to strain rate effects, being almost twice as susceptible as the next ranking material, namely, the HF-1 steel alloy having a tempered martensitic microstructure with grain boundary network (Type 1). In contrast, the 52100 steels, for both the embrittled and normalized conditions, were least affected by strain rate variations.

2. Both the yield and tensile strengths increased with increasing strain rates for the 4340 (Q&T) steel; the HF-1 steel, in the three heat-treated conditions; the two titanium alloys (6Al-6V-2Sn and 6Al-4V); and the uranium alloy (8Mo-1/2Ti). The yield strength of the 52100 steel in the high-temper grain boundary embrittled (IQ&T) condition decreased moderately with strain rate, whereas in the normalized (Norm&T) condition the reverse was true, i.e., a moderate increase was noted as the strain rate increased. The tensile strength of this 52100 alloy, in both the embrittled and normalized conditions, exhibited a relatively constant value over the strain rates investigated.

3. True fracture stress increased markedly with increasing strain rate for the two titanium alloys, the uranium alloy, and Types 2 and 3 of the HF-1 steel. The remaining steel alloys: HF-1 (Type 1), 52100, in both the embrittled and normalized conditions, and the 4340 (Q&T) maintained a fairly constant strength level over the strain rates examined.

4. The modulus of elasticity in tension increased significantly with strain rate for the U-8Mo-1/2Ti alloy, the 4340 (Q&T) alloy, and the HF-1 steel in the three heat-treated conditions. The modulus value behaved linearly for all three types of HF-1 steel with the rate of increase being approximately equivalent for all conditions. However, for the 4340 steel and the gamma-stabilized uranium alloys, the increase in the tension modulus was moderate from quasi-static to approximately  $1.0$  to  $3.0 \text{ sec}^{-1}$  with a marked increase occurring at strain rates above this transition range. The 52100 steel, in the grain boundary high temper embrittled (IQ&T) and normalized (Norm&T) conditions, was relatively insensitive to strain rate as evidenced by the fact that the modulus response was essentially flat with respect to strain rate. In the case of the titanium alloys there was a contradiction of results; for the 6Al-6V-2Sn alloy the modulus increased moderately with increasing strain rate, whereas the 6Al-4V alloy exhibited a decrease in this characteristic with strain rate.

5. The ductility, as measured by the reduction of area, varied essentially monotonically with strain rate for all the alloys tested except U-8Mo-1/2Ti. A marked loss in ductility was noted for this uranium alloy when the strain rate increased from approximately  $10^0$  to  $5 \times 10^2 \text{ sec}^{-1}$ .

6. The U-8Mo-1/2Ti alloy was the material most sensitive to strain hardening behavior, wherein a significant decrease in the strain hardening index occurred with increasing strain rate thereby signalling the development of a softening process. This phenomenon was peculiar to all the materials evaluated with the exception of the 52100-2 (IQ&T) alloy which exhibited an increase in the strain hardening slope with strain rate thereby indicating the development of a strain hardening mechanism. Least influenced was the 52100 steel in the normalized condition which remained neutral to strain hardening effects displaying no change in the strain hardening index with strain rate. The titanium alloys and the two HF-1 steel alloys (Types 2 and 3) showed a significant increase in flow stress but no apparent change in fracture behavior.

The following summarizations are made on the effect of strain rate on mechanical properties of selected alloys at various test temperatures within the limits of the strain rates studied for  $10^{-3}$  to  $5.3 \times 10^2 \text{ sec}^{-1}$ :

1. For the HF-1 steel, in the three heat-treated conditions at the test temperature of -116 C (-175 F):

a. Yield strengths were sensitive to strain rate; the strength levels for all three conditions increased moderately with increasing strain rate. For Types 1 and 3, these values paralleled and were slightly higher than those observed at room temperature; for Type 2 the levels obtained were significantly greater than room temperature results particularly at high-order strain rates.

b. The tensile strength and true fracture stress were unaffected by strain rate. The values at the subzero temperature remained constant over the strain rates examined and were inferior to room temperature results at relatively high-order strain rates, the degradation in performance becoming progressively greater as the strain rate exceeded approximately  $30 \text{ sec}^{-1}$  in the case of the true fracture stress and  $10^2 \text{ sec}^{-1}$  for the tensile strength.

c. The modulus of elasticity in tension was quite sensitive to strain rate, particularly for the high strength-high ductility conditions (Types 1 and 2) which increased markedly with increasing strain rates. The tension modulus determined for the high strength-high ductility tempered martensite steel (Type 1) was much higher than the corresponding values obtained at room temperature, particularly at the high strain rates, in contrast to the results with the low strength-low ductility coarse pearlitic specimens (Type 3) wherein the modulus was sharply attenuated throughout the rate range investigated.

d. Based on the limited data available, ductility was hardly affected by strain rate except for the incompletely austenitized condition (Type 1) which exhibited a pronounced decrease in ductility with increasing strain rate. In comparison with the room temperature data, a severe loss in ductility was noted in all cases.

e. In general, the strain rate sensitivity decreased as the temperature decreased from +23 C to -116 C with Type 3 being least affected by strain rate variations.

f. At low-order strain rates, the temperature influence on the mechanical property results of Type 3 material was approximately 64% greater than that of Type 1. The temperature interaction resulting at high-order strain rate conditions, even though the levels of susceptibility were higher than those attained at low-order strain rates, was quite comparable for all three types. At high-order strain rate conditions the three types of HF-1 steel were ranked in the following descending order of susceptibility to the subzero temperature change: Types 1, 3, and 2. For the alloy having the tempered martensitic microstructure with grain boundary network (Type 1) the temperature effects at high-order strain rates were approximately twice (1.94) that occurring at low-order strain rates. However, temperature effects on the alloy in the isothermally transformed to coarse pearlite microstructure (Type 3) were relatively independent of strain rate wherein a negligible difference of only 5% was realized.

g. The incipency of a softening process was revealed for all three types of this material. The strain hardening characteristic  $n$  for each type decreased significantly with increasing strain rate; as a consequence of the differences encountered in the rates of change in the strain hardening characteristics, Types 3, 2, and 1 were ranked in descending order of sensitivity with respect to strain hardening behavior.

h. Analysis of the influence of the subzero temperature on the strain hardening phenomenon exposed the negligible temperature effects on Type 1 in contrast to the dramatic sensitivity exhibited by Types 2 and 3. Type 3 was extremely sensitive to the subzero environment wherein the strain hardening characteristic decreased by a factor of 47 relative to room temperature results.

2. With respect to the performance of the 8Mo-1/2Ti uranium alloy at test temperatures from -73 C to 260 C:

a. Yield strength, tensile strength, and true fracture stress were quite sensitive to strain rate; all strength values, independent of temperature, varied with increasing strain rate in a consistent manner. Within the temperature and strain rate spectrum investigated, all strength levels, at constant strain rates, increased continuously with decreasing temperature.

b. Overall, the tension modulus was significantly influenced by strain rate variations. The modulus of elasticity, independent of temperature, increased with increasing strain rate. At low-order strain rates, from quasi-static to approximately  $3.0 \text{ sec}^{-1}$ , the modulus increased moderately at all test temperatures, the rate of increase being relatively proportional; for the higher strain rates up to  $530 \text{ sec}^{-1}$  the modulus increased markedly at temperatures from -73 C to 149 C, whereas at 260 C it was essentially neutral. At strain rates above  $3.0 \text{ sec}^{-1}$ , the rate of increase of the modulus became more pronounced as the temperature decreased from 260 C to -73 C.

c. Ductility was critically dependent on strain rate as well as temperature. At each temperature level, with the exception of 260 C where an incremental increase was noted, the loss in ductility was more pronounced at the high orders of strain rate. The degradation in ductility from the temperature variation contribution exceeded that caused by the strain rate effects alone, under maximized conditions, by a factor of approximately 3:1.

d. The effect of temperature on the strain rate sensitivity of this gamma-stabilized alloy decreased as the test temperature decreased with a negligible change (5.7%) occurring from +149 C to +23 C. As the temperature increased from +23 C to +260 C, the strain rate influence increased by approximately 80%, whereas from +23 C to -73 C there was a decrement of approximately 50% in the sensitivity indicator.

e. The extent of temperature effects, at constant strain rate, on the mechanical property results indicated that the temperature influence, under quasi-static strain rates, remained fairly constant as the temperature either increased from +23 C to +149 C or decreased to -73 C but a moderate change (38%) was realized when the temperature increased to +260 C. In comparison with the low-order strain rate results, the temperature effects, under dynamic loading rates, were much more pronounced at elevated test conditions, whereas a relatively modest change occurred at the subzero temperature.

f. As a result of the elevated and subzero temperature input, under low-order strain rate conditions, a strain hardening mechanism predominated, whereas at high magnitudes of strain rate the development of a softening process prevailed. At low-order strain rates, the following conclusions can be drawn pertaining to the influence of elevated and subzero temperature changes on strain hardening behavior: (1) an approximate threefold increase in strain hardening was incurred at the subzero temperature of -73 C; (2) a substantial 51% decrease in strain hardening was realized at the elevated temperature of +149 C; and (3) a relatively insignificant change (7.6%) occurred at +260 C. At high-magnitude strain rates, strain hardening was drastically reduced by a factor of the order of 4.0 to 4.6 at both elevated temperatures; in contrast, at the subzero temperature there was an approximate 125% increase in the strain hardening characteristic.

#### ACKNOWLEDGMENT

Acknowledgment is made of the invaluable assistance rendered by Mr. Paul V. Riffin, Engineering Mechanics Division, Army Materials and Mechanics Research Center, for his recommendations of the pertinent metallurgical processing treatments given and for providing all the test materials employed in this experimental evaluation program.

# APPENDIX A. TABULATION OF TEST DATA AND TRUE STRESS-TRUE STRAIN RESULTS

Table A-1. EXPERIMENTAL TEST DATA AT ROOM TEMPERATURE

Material	Test Spec.	True Fract. Stress (ksi)	Ult. Str. (ksi)	Yield Str. (ksi)	Strain Rate (sec <sup>-1</sup> )	Tension Modulus 10 (psi)	R.A. (%)
4340 Steel (Q&T)	1	255	156	138	0.0079	30.8	59.5
	2	225	148	130	0.0070	31.2	59.1
	3	267	155	135	0.0081	30.8	60.3
	4	-	160	141	1.18	32.9	62.8
	5	247	163	141	0.85	32.2	51.2
	6	242	158	145	1.18	33.0	60.3
	7	234	161	149	36.	36.1	61.2
	8	248	173	158	52.	38.6	60.3
	9	248	-	159	36.	37.6	60.3
52100 Steels	-1 (IQ&T)	1	190	178	-	4.	14.0
		2	191	164	-	60.	17.9
	-2 (IQ&T)	1	224	-	186	1.7	31.0
		2	220	179	179	0.004	30.9
		3	-	186	123	3.1	30.8
		4	227	182	146	55.	30.4
		5	204	164	-	68.	20.1
	-3 (Norm&T)	1	208	185	146	0.004	30.8
		2	207	189	97	1.9	-
		3	203	190	103	2.8	-
		4	-	-	-	-	-
		5	206	178	-	41.	-
		6	213	166	153	33.	30.7
	Ti-6Al-4V	5	218	168	158	0.004	20.4
		2	200	167	158	.017	20.4
		7	205	168	164	2.4	19.5
		4	220	174	167	3.8	20.6
		12	218	172	164	10.	19.8
		6	234	183	171	27.	19.1
		3	229	184	169	50.	19.1
		9	256	216	-	88.	-
		10	252	205	-	68.	-
		11	271	212	-	109.	-
		16	218	-	174	0.010	18.7
Ti-6Al-6V-2Sn	17	212	-	174	.014	19.4	19.0
	24	244	207	189	.015	19.8	25.8
	14	233	186	-	2.1	-	31.3
	13	244	180	-	21.	-	26.8
	22	238	212	204	9.2	21.3	30.2
	18	264	261	211	136.	20.3	31.2
	20	249	235	207	60.	20.7	36.8
	21	280	233	-	120.	-	33.5

Preceding page blank

Table A-2. EXPERIMENTAL TEST DATA TAKEN AT VARYING TESTING TEMPERATURES

Material	Test Temp. (deg C)	Test Spec.	Fract. Stress (ksi)	Ult. Str. (ksi)	Yield Str. (ksi)	Strain Rate (sec <sup>-1</sup> )	Tension Modulus 10 <sup>3</sup> (psi)	E.L. (%)
AISI Steel								
Type 1	23	1-12	226	162	103	1,503	31.2	22.4
		1-8	218	161	136	1,502	31.4	22.1
		1-10	223	187	155	1,505	32.3	21.9
		1-5	210	180	-	1,719	-	22.2
		1-11	-	-	-	-	32.5	22.4
		1-1	219	188	146	1,121	34.5	22.1
		1-4	215	182	154	49	33.8	25.9
		1-13	-	-	186	408	31.7	35.5
		1-2	232	197	195	445	46.2	29.2
	-116	1-3	219	249	187	358	33.8	12.1
		1-6	232	194	163	9,19	33.2	21.5
		1-9	196	192	175	420	35.9	-
		1-7	215	197	179	-	-	10.9
Type 2	23	2-2	202	169	123	1,901	31.2	24.1
		2-3	216	177	124	1,902	31.5	24.9
		2-7	212	179	124	1,908	31.7	24.3
		2-5	244	187	143	1,560	33.6	36.3
		2-6	261	210	134	4,129	34.4	31.6
		2-9	250	201	128	27.2	34.6	26.9
		2-1	-	-	-	32.3	35.1	27.3
		2-8	278	210	158	539	36.2	28.9
	-46	2-15	213	-	169	251	34.6	12.5
		2-12	-	201	146	1,173	34.1	-
	-116	2-11	235	203	169	245	39.5	15.9
		2-19	236	199	171	516	39.8	15.7
Type 3	23	3-12	163.5	145.9	74.4	1,102	30.6	11.1
		3-15	163.6	149.4	74.6	1,003	31.1	9.8
		3-3	183.7	169.1	95.7	1,510	32.9	7.9
		3-7	195.0	176.0	102.4	4,64	32.8	9.7
		3-6	185.2	167.9	99.1	40.6	33.1	8.8
		3-2	198.4	185.6	118.9	186	35.9	9.3
	-62	3-13	160.6	156.4	112.1	306	33.2	1.6
		3-8	168.9	162.4	99.2	1,054	31.6	3.8
	-116	3-10	-	-	100.0	1,124	31.7	6.8
		3-1	170.4	163.0	123.7	340	32.8	4.3
AISI 1020	260	4-4	110	72	64	1,001	13.6	51.9
		3-4	104	69	64	1,006	12.3	46.2
		2-4	123	92	95	1,15	15.3	50.6
		7-2	137	90	88	1,19	15.6	56.7
		5-2	124	136	192	531	13.5	12.7
		4-1	-	-	-	501	14.3	54.3
	143	6-4	150	97	91	1,108	10.1	53.5
		3-3	138	72	82	1,008	11.7	53.3
		4-3	153	115	109	1,17	12.9	49.2
		7-4	151	116	111	3,4	11.5	48.1
		4-1	159	194	194	277	17.6	35.4
		5-2	148	191	191	176	14.5	32.1
		5-1	-	-	-	-	-	37.0
	73	1-4	171	134	121	1,014	12.3	41.6
		6-1	154	131	122	1,014	12.2	38.1
		7-1	167	163	155	1,15	16.3	41.6
		3-1	174	164	158	5	14.7	33.1
		1-2	208	203	196	406	14.3	10.3
		4-4	212	215	208	535	18.7	21.4
	-73	6-2	168	170	155	1,014	12.0	10.3
		1-2	190	172	150	1,016	12.2	26.3
		1-3	202	176	165	1,4	14.7	9.9
		5-3	215	181	170	1,4	14.9	13.1
		4-2	291	-	-	-	-	7.9
		2-1	238	245	204	227	20.3	5.4

Table A-2. True Stress-Strain Relationship at Room Temperature

Material	True Strain (in./in.)	True Stress (ksi)	Strain Rate (sec. <sup>-1</sup> )	True Strain (in./in.)	True Stress (ksi)	Strain Rate (sec. <sup>-1</sup> )
A340 Steel (Q&T)	0.0045	175	0.0029	0.00430	141	0.845
	0.0058	185	0.0029	0.0067	164	0.845
	0.004	155	0.0029	0.0046	247	0.845
	0.00417	110	0.0020	0.0044	135	1.18
	0.0291	140	0.0020	0.0205	158	1.18
	0.042	225	0.0020	0.025	242	1.18
	0.0430	135	0.0081	0.0041	149	36.4
	0.0152	155	0.0081	0.0230	161	36.4
	0.025	267	0.0081	0.046	234	36.4
	0.00439	141	1.18	0.0041	158	52.5
	0.006	160	1.18	0.0066	173	52.5
	0.0042	159	36.5	0.025	242	52.5
	0.025	246	36.5			
52100 Steels						
Ti-6Al-4V						
Ti-6Al-6V-2Sn						

Table A-4. TRUE STRESS-TRUE STRAIN RESULTS TAKEN AT VARYING TESTING TEMPERATURES

a. HF-1 Steel									
Test Temp. (deg C)	Type 1			Type 2			Type 3		
	True Strain (in./in.)	True Stress (ksi)	Strain Rate (sec <sup>-1</sup> )	True Strain (in./in.)	True Stress (ksi)	Strain Rate (sec <sup>-1</sup> )	True Strain (in./in.)	True Stress (ksi)	Strain Rate (sec <sup>-1</sup> )
23	0.0030	103.0	0.003	0.0039	123.2	0.001	0.0026	74.6	0.002
	.0625	172.7	.003	.2754	202.2	.001	.0476	153.0	.002
	.3920	226.0	.003	.0037	124.3	.002	.1178	163.5	.002
	.0044	136.2	.003	.0653	188.4	.002	.0025	74.6	.021
	.0700	172.8	.003	.3535	216.1	.002	.0540	157.7	.021
	.3293	218.0	.003	.0041	129.6	.008	.0926	163.8	.021
	.0037	155.8	.583	.2792	212.2	.008	.0024	90.9	.510
	.0583	198.0	.583	.0037	143.2	.560	.0536	178.4	.510
	.3839	223.1	.583	.0594	198.5	.560	.0825	183.7	.510
	.0618	191.5	.719	.4504	243.7	.560	.0931	180.7	4.64
	.3045	210.4	.719	.0031	134.1	4.29	.0041	187.6	4.64
	.0043	147.0	5.21	.0618	223.5	4.29	.1026	195.0	4.64
	.0641	200.2	5.21	.3805	250.0	4.29	.0024	99.3	40.6
	.3577	218.5	5.21	.0061	156.7	532.	.0720	175.1	40.6
	.0043	154.2	49.	.0720	225.3	532.	.0926	185.2	40.6
	.0594	192.9	49.	.3408	252.6	532.	.0034	118.4	286.
	.3053	214.6	49.	.0037	128.4	27.2	.0606	197.2	286.
	.0055	170.0	408.	.0224	205.9	27.2	.0980	198.4	286.
	.0049	185.6	445.	.3134	241.8	27.2			
	.0675	210.8	445.						
	.250	231.5	445.						
-46				0.0049	170.1	252.			
				.1340	212.8	252.			
-62							0.0034	112.1	306.
							.0212	159.7	306.
							.0266	160.6	306.
-73	0.0055	187.5	320.						
	.1293	218.7	320.						
-116	0.0049	164.1	9.19	0.0043	147.0	2.23	0.0031	100.1	2.04
	.2422	231.8	9.19	.0426	209.4	2.23	.0331	168.0	2.04
	.0061	175.8	420.	.0043	170.0	245.	.0392	168.9	2.04
	.116	214.7	420.	.0373	210.9	245.	.0031	100.3	2.24
				.174	241.7	245.	.0037	124.2	340.
				.0043	171.6	516.	.0402	169.7	340.
				.1237	225.7	516.	.0440	170.4	340.
				.171	236.4	516.			

Table A-4. (Cont'd)

b. Uranium Alloy 8Mo-1/2Ti						
Test Temp. (deg C)	True Strain (in./in.)	True Stress (ksi)	Strain Rate (sec <sup>-1</sup> )	True Strain (in./in.)	True Stress (ksi)	Strain Rate (sec <sup>-1</sup> )
260	0.0149	192.9	531.	0.837	137.1	1.85
	.749	124.2	531.	.00499	64.4	.0053
	.00654	95.9	2.50	.1506	87.6	.0053
	.00748	100.0	2.50	.7319	115.9	.0053
	.705	122.6	2.50	.00499	64.3	.00565
	.00623	88.1	1.85	.1750	82.0	.00565
	.00748	90.9	1.85	.6200	104.5	.00565
149	0.0135	196.6	277.	0.01124	93.1	0.00814
	.437	158.5	277.	.7617	138.1	.00814
	.0130	197.0	176.	.0075	110.1	3.71
	.387	148.5	176.	.0091	115.5	3.71
	.00748	91.5	.00795	.825	153.3	3.71
	.00995	97.7	.00795	.00837	111.6	3.37
	.7659	150.0	.00795	.0103	117.3	3.37
	.00748	88.2	.00814	.500	131.0	3.37
23	0.0124	156.6	2.45	0.00936	122.1	0.014
	.0134	162.4	2.45	.018	135.1	.014
	.538	186.6	2.45	.5412	170.8	.014
	.0117	160.2	5.	.00995	199.5	406.
	.0134	166.3	5.	.0344	209.7	406.
	.401	174.4	5.	.131	207.7	406.
	.00995	123.4	.0*	.0124	210.7	333.
	.0124	132.3	.014	.0173	222.1	333.
	.4367	154.0	.014	.241	211.6	333.
-73	0.0087	206.0	227.	0.3045	189.8	0.016
	.0554	237.8	227.	.0161	168.0	1.39
	.0135	167.4	.015	.0165	179.3	1.39
	.198	174.3	.015	.1247	201.9	1.39
	.1089	158.3	.015	.0161	173.2	1.42
	.0135	170.8	.016	.0164	184.4	1.42
	.0198	177.7	.016	.225	215.2	1.42